#3426

FINAL REPORT - 1988

INVESTIGATION OF RADON ENTRY INTO DWELLINGS AND THE EFFECTS OF SELECTED RADON MITIGATION TECHNIQUES

Sponsored by

The United States Environmental Protection Agency
Air and Energy Engineering Research Laboratory
Research Triangle Park, North Carolina
Project Officers: David Sanchez and Ronald Mosley
Contract Number CR-814673-01-4

and The New Jersey Department of Environmental Protection
Project Officer: Arnold Wickland
Purchase Order Number 25876

by

Lynn M. Hubbard, Benjamin M. Bolker, Kenneth J. Gadsby,
David T. Harrje, and Robert H. Socolow

Center for Energy and Environmental Studies
Princeton University
Princeton, N.J. 08544-5263

December 1988

Table of Contents

The sections of this final report each include their own references and figures.

PART A. Radon Dynamics in a House Heated Alternately by Forced Air and by Electric Resistance

Summary 1
Introduction 2
Data Collection 3
Variations in Heating Conditions 4
Flow Mode 8
HAC Interaction 11
Conclusion 12
References 13
Appendix A: Pressure versus Flow Calculation 15
Appendix B: Budget Calculation: Airflow and Entry 22
Figures 25

PART B. Rapid Diagnostics: Subslab and Wall Depressurization Systems for Control of Indoor Radon

Introduction 36
Connectivity 38
Testing Protocol 38
Princeton Pre-Mitigation Rapid Diagnostics Protocol 38
Equipment Needs for Connectivity Testing 41
Example of Choosing the SSD Mitigation Suction Location . . 42
Pressure Differences Under Various House Conditions 42
Pressure Field Extension 43
Flow 44
Conclusions 45
References 45
Tables and Figures 47
Appendix: Additional Diagnostic Measurements 53
Figures 55

PART C. An Approach to Measuring Durability in Radon Mitigation Systems

Background 59
Data Collection 59
Radon Data Evaluation 62
Pressure and Velocity Data 64
Conclusions 65
Tables 67
References 70

PART A - RADON DYNAMICS IN A HOUSE HEATED ALTERNATELY BY FORCED AIR AND BY ELECTRIC RESISTANCE

SUMMARY

Understanding the various mechanisms driving radon entry into buildings aids in the development of appropriate diagnostic measurement techniques and in the design of efficient mitigation systems. Environmental parameters such as temperature, wind, and rainfall, and house specific parameters such as type of heating and cooling system, leakiness of the house to outside air, and leakiness of the sub-structure to the soil gas provide the driving forces and conditions for radon entry. This report presents field data, analysis, and modeling which describe the effect of central heating air distribution systems and electric heating systems on air infiltration into buildings, movement of air and radon around buildings, and the rate of entry of radon-containing soil gas into buildings. The interaction of central air distribution systems with subslab depressurization systems is also included in the discussion.

I. INTRODUCTION

Several mechanisms are responsible for the time dependent variations in radon entry into buildings as a result of pressure driven flow. The dominant mechanisms are the "stack effect" (driven by temperature differences between the indoors and the outdoors), the effect of wind on the building shell, and the operation of mechanical ventilation systems which distribute heated or cooled air throughout the house. The rate of radon entry into indoor air also varies with weather conditions, such as rain, which alter the soil conditions and thus the flow of soil gas through the soil to the building shell(1,2).

The Piedmont study conducted in New Jersey during 1986-87 and follow-up studies during 1987-88 have provided an extensive data set for analyzing relationships between weather and house specific variables and radon behavior indoors(1,2). These relationships have contributed to the early stages of development and verification of a model which incorporates physical mechanisms for radon entry. The Piedmont data, however, are limited to forced-air heating systems. In order to clarify the role of the heating system, we performed research this past year at an additional house where we were able to vary the method of heating between forced air with a gas combustion furnace and electric resistance heating. This report discusses the interesting relationships between radon entry and house dynamics which have emerged from this research.

We have two kinds of modeling efforts:

1. Heuristic modeling: a) to determine which house parameters are most important in driving radon entry, b) to determine if there is a house signature, some small set of quantities which are easy to measure, which can characterize the radon problem of the house, and c) to determine the variability of soil gas entry from house to house.

2. Predictive modeling: a) to predict, given (by the modeling above) a few measured parameters from a house, the type of mitigation system best suited for the house, and b) to determine the relationship between short term and long term data; for example, can time series measurements taken in a house for one week in December be used to determine an annual average radon exposure?

These are long-term goals. The following discussion represents the results of a first step in this development process.

This report is organized as follows. Section II describes the house and data used in this study, along with various techniques for estimating and measuring the radon entry rate, airflows, and radon

concentrations in different parts of the house. Section III discusses the characteristic behavior of the radon and airflow dynamics during different types of heating periods, including an estimate of the minimum and maximum bounds on the flow of soil gas into the basement. Section IV concludes with a discussion of an interzone flow model, with calculations of radon concentration and entry rate, and the how use of an air distribution system is incorporated in the flow model.

II. DATA COLLECTION

The data used in this study come from research house PU21. The house is a single-story ranch style house with a basement under one third of the total floor area of the house and a slab under the rest of the house. The basement has hollow cinder block walls, a floor drain communicating with the outside in the center of the basement slab, and a perimeter floor-wall crack.

Data description. The data consist of half-hourly measurements of temperatures indoors and outdoors, pressure differentials across the basement shell, heating and air conditioning (HAC) system use, outdoor weather variables, radon concentrations at several points around the test house, and tracer gas airflow measurements. The temperature, pressure, HAC, and weather measurements are part of our routine data collection at test houses, and are consistently available for all time periods. Continuous radon measurements are also routine for the basement, upstairs, and subslab, while wall radon measurements are intermittently available.

Tracer gas system. The airflow data come from a multiple tracer mass spectrometer (MTMS) system developed at Lawrence Berkeley Laboratory(3,4). The MTMS system emits different tracer gases in several zones, measures the concentrations of the gases in each zone, and uses a mass balance equation to calculate the flow between all zones and between zones and the outdoors continuously for specific time periods. The experimental error in the MTMS data varies between the two heating periods used in this report. During gas combustion, the average error was 2% for infiltrations and 10% for interzone flows, while during electric heat the errors were 8% for infiltrations and 15% for interzone flows. The error was always at least 5 m^3/hr for infiltrations and 10 m^3/hr for interzone flows(5).

Radon entry rates. Tracer gas emissions and concentration data can be used to calculate radon entry rates as well as airflows within houses. We have previously shown that, if we assume that the tracer gas emitted in the basement zone behaves the same as radon, the ratio of tracer gas emission to tracer gas concentration should be equal to the ratio of radon entry rate into the basement to radon concentration in the basement. Thus, knowing the tracer gas emission rate and concentration and the radon concentration in the basement, we can calculate the radon entry rate(6). The MTMS system can produce the data we need for this calculation.

III. VARIATIONS IN HEATING CONDITIONS

Experiments. Research house PU21 was the site of experiments to compare the radon entry rate and the distribution of radon indoors during different heating conditions. The experiments involved heating the house alternately with electric resistance heaters installed on the living levels and with a gas combustion unit in the basement connected to a whole house air distribution system, sometimes called an air handler. The gas combustion furnace and air handler heating system usually runs on an automatic setback mode, during which the thermostat automatically sets back to 55°F (13°C) at midnight and turns back up to its previous setting at 8 AM. The data show that the air handler has a large effect on pressure differences across the building shell, and on the distribution of the radon indoors. We will compare these effects to the time periods when the air handler was not operating.

Figure 1 shows the radon concentrations, measured each half hour, in the basement and in the subslab during a gas combustion with automatic setback (GC) period along with the pressure differences between the outdoors and the basement and between the subslab and the basement, and the percent time the air handler is on during each half hour. Figure 2 shows the same parameters for an electric heat (EH) period. The sharp rises in the pressure differences in Figure 1 coincide with the time the air handler is on. During the same periods, the basement radon decreases while the subslab radon increases. Increased mixing of the basement air with the upstairs air by the air handler causes the decrease in basement radon concentration. The variation in the upstairs radon during the air handler use, not plotted in Figure 1, closely parallels the pattern of the subslab radon concentration, and the upstairs radon increases by roughly the amount of radon the basement loses. (These patterns are quantified in Table 1.)

Air handler and pressure changes. Operation of the air handler is the main driving force for the variation in the radon concentration during GC. The air handler increases the pressure difference between the basement and the outdoors by 1.8 Pa, and between the basement and the subslab by 0.9 Pa; the mechanism for the pressure changes will be explained in section V of this report. The increased pressure difference increases the air infiltration into the basement. This increased air infiltration includes both soil gas and outdoor air. Each house will have a different ratio between the degree of leakiness to the soil gas and the degree of leakiness to the outdoors. This ratio determines whether increased air infiltration raises or lowers the indoor radon concentration. If, for example, the basement is very leaky to outdoor air but fairly well isolated from the soil gas, outdoor air will make up most of the increased infiltration and thus dilute the basement radon. It would be helpful to know how much this quantity varies among different houses. If it remains relatively constant among similar housing types on soils with similar permeabilities, it may be possible to design a measurement to characterize the potential radon problem on a building site based on

the soil permeability and radon content. However, there is no indication in our research yet that the flow into buildings from the soil gas is similar in similar houses (6), although there are not yet many data to compare.

Statistical analysis. During the electric heating (EH) period, shown in Figure 2, the basement radon concentration lags the subslab radon concentration by about 2.5 hours, based on cross correlations computed at different lags. Regression analysis shows that the pressure differences (shown in the bottom plot) vary primarily because of the temperature difference between the indoors and outdoors, which causes a stack pressure of varying magnitude. A linear regression applied to the radon data from the EH period gives a good fit of the basement radon concentration ([Rn]) as a function of the radon in the subslab lagged 2.5 hours behind the basement radon, the temperature difference between the indoors and outdoors, and an intercept, or baseline radon concentration:

$$[Rn]_{basement} = 36\ (\pm 8)\ pCi/L + 0.10\ (\pm 0.003)\ [Rn]_{subslab,\ t-2.5\ hrs} + 7.7\ (\pm 0.5)\ pCi/L/^{\circ}C\ \Delta T$$

$r^2 = 0.74$

residual standard error = 42 pCi/L

A possible explanation for the 2.5 hour lag between subslab and basement radon is the relatively slow rate of convective flow from the subslab to the basement.

During the GC heating period, the best statistical fit for predicting radon in the basement, as a function of radon in the subslab, temperature difference between the indoors and the outdoors, and air handler time on, had a coefficient of determination (r^2) of only 0.17. The use of the air handler results in a poorly correlated time variation of the basement and subslab radon concentrations if several days of data are evaluated together. If only a single day of time series data is evaluated, however, the above parameters predict radon quite well. The intercept in the fit of basement to subslab radon varies considerably from day to day, which degrades the regression for the longer time period. We are currently trying to find the cause of this variation, which is absent during the electric heating period.

Consider the time it takes for the subslab and basement radon to return to equilibrium--that is, a condition (such as the condition associated with the electric heating period, represented in Figure 2) unaffected by both the redistribution of basement air and increased basement air infiltration caused by the depressurization of the basement during the air handler use associated with the GC heating period. During the GC heating period, the air handler was off every night between midnight and 8 AM. Figure 1 shows that the basement radon concentration rises during these times while radon flow into the basement depletes the subslab radon. Figure 3 shows similar behavior in the wall; radon is depleted when the air handler is on and returns when the air handler shuts off. During the 8 hours that the air

handler is off, though, the basement and subslab radon concentrations do not return to a condition where they are again correlated with temperature difference and subslab radon concentration, as in the electric heating period. In this house, therefore, the time it takes to return to a condition unperturbed by the pressure differences caused by the air distribution system is longer than 8 hours. This time is related to the radon availability to the subslab soil gas reservoir from the surrounding soil.

Hollow block walls. The interiors of hollow block walls can be an important reservoir for radon (7), so it is important to understand radon behavior in walls under different heating conditions. Figure 3 shows wall radon concentrations at house PU21 during a 3-day period in the spring. Until day 97.375 (Julian day 97 at 0900), the HAC system stays off and the wall concentrations show a smooth daily cycle caused by the outdoor temperature cycle and the stack effect. When the HAC system comes on, it suddenly depletes the radon concentration in the walls. When it goes off the following night during setback, the radon concentration rises to its previous level or higher. During 2 days (Julian days 100 and 101) when the average outdoor temperature, 10.3 ^{o}C, was comparable to the non-heating period average outdoor temperature of 12.8 ^{o}C, the average wall radon level was 880 pCi/L, significantly higher than the non-heating period average of 530 pCi/L. Thus, the average wall radon concentration appears to rise during periods of HAC operation.

Heating period averages. Table 1 presents averages of the measured data from house PU21 during the GC and EH heating periods. Both heating periods are during the middle of winter, with similar indoor and outdoor temperatures. This minimizes the difference in the contribution to indoor radon between the two periods due to the stack effect, so that the main difference between the two periods is the effect of the air handler on air and radon distribution, as discussed above. Table 1 shows the increased mixing of indoor air during GC; note the eightfold increase in basement to upstairs flow during the GC heating period and the two to threefold increase in upstairs to basement flow. Radon levels also indicate increased mixing during GC. The distribution of indoor radon changes; much more radon remains in the basement during EH (302 pCi/L) than during GC (245 pCi/L). As a result, the upstairs radon concentration during GC (112 pCi/L) is a little more than double the amount during EH (51 pCi/L). Understanding how heating systems affect the distribution of the radon indoors is an important factor in determining how the health risk associated with exposure to radon varies between houses.

Table 1 also shows that the radon entry rate, obtained as described in Section II using the emission rates and concentrations of the MTMS tracer gas, is higher during the GC period than during the EH period. Radon entry rate is a function of radon concentrations in the subslab and wall reservoirs around the basement and the flows from those reservoirs into the basement. The redistribution of air in the air handler during GC heating depressurizes the basement, which both

pulls radon from the surrounding soil into the subslab gravel bed and the interior of the block walls and increases the flow from those areas into the basement. Figure 4 displays data from Table 1; the average radon concentrations and pressure differences (relative to the basement) during the two heating periods are compared. The average subslab radon concentration rises from 1460 to 2077 pCi/L during GC. Wall radon concentrations stay the same or rise slightly during GC, as shown in Figure 3. Measuring flows from the soil gas reservoirs into the basement is quite difficult, but the 0.8 Pa increase in subslab-basement pressure differential and the 26 m^3/hr increase in basement infiltration, some of which represents soil gas, both indicate an increase in pressure-driven flow of soil gas into the basement. Decomposing the radon entry rate into a flow term and a concentration term by making more extensive flow and concentration measurements in the basement would be a useful future project.

Bounds on soil gas flow into the basement. Although the flow and concentration terms cannot be obtained explicitly, the data available from these experiments do give us upper and lower bounds for the flow from the soil gas to the basement. We know the flow from the soil gas is some fraction of total flow into the basement, which is made up of flow from the outdoors to the basement plus flow from the soil gas to the basement. Thus, the upper bound is simply the total measured flow from the outside to the basement. The total flow into the basement, or infiltration, is plotted as a dotted line in the lower box of Figure 5.

The minimum flow from the soil gas into the basement can be obtained by recalling that the radon entry rate equals the average radon concentration in the soil gas flowing into the basement times the flow rate of the soil gas. We know the total radon entry rate, obtained from the MTMS tracer gas system as explained in Section II, and plotted in the top box of Figure 5. We do not know the average radon concentration in the soil gas flowing into the basement, which would require several simultaneous and continuous measurements of the radon content of incoming soil gas. Of the variety of grab samples of soil gas obtained from different locations under the slab and in the hollow block wall cavities, the location where the continuous monitor was measuring consistently had the highest radon concentration. (The subslab concentrations plotted in Figures 1 and 2 were measured at that point.) It is thus a safe assumption that the continuously monitored subslab radon is an upper limit for the average radon concentration in the inflowing soil gas. Dividing the radon entry rate plotted in the top of Figure 5 by this maximum radon concentration, we obtain the minimum flow from the soil gas plotted as a solid line in the bottom of Figure 5. Surprisingly, the average of the minimum flow is 20% of the average of the total flow measured from the outside into the basement. Thus, this analysis shows that more than 20% of the total flow into the basement is from soil gas!

Equilibrium ratio. Table 2 compares the measured radon progeny concentration (using continuous working level monitors) with the radon

gas concentration in the upstairs and the basement during the two heating periods. Also shown is the equilibrium ratio between the average progeny and radon concentrations. The equilibrium ratio remains relatively constant during the two heating periods, implying the progeny behaves similarly to the radon gas. We consistently measured a higher equilibrium ratio in the upstairs than in the basement, regardless of the heating system. Several mechanisms could contribute to this effect. We have observed more aerosols in the upstairs air than in the basement air in this research house (8). This imbalance could account for the increased equilibrium ratio upstairs, since increased aerosol content of the air increases the number of airborne progeny attachment sites. During GC heating, however, the upstairs aerosols would be expected to be mixed with the downstairs air, thus diluting the airborne progeny content upstairs and increasing it downstairs. We do not observe these changes, but these effects may be countered by the high basement radon levels being redistributed intothe upstairs air by the air handler. Another mechanism for the high equilibrium ratio upstairs is that the air entering from the basement may already contain progeny in significant amounts, whereas the air entering the basement contains radon gas with no progeny. It is also likely, however, that air forced upstairs from the basement through the air handler would have its progeny levels reduced because of plating out in the duct system and on the filters. Ongoing analysis using the radon zone models and the time-dependent progeny model (8), along with more extensive aerosol and progeny measurements in the research house, should teach us more about the dominant mechanism responsible for the observed larger percentage of progeny relative to radon upstairs.

IV. FLOW MODEL

The flow model is a simple zone model which uses radon flows around a house to predict radon concentrations in each zone. The model currently uses three zones to simulate radon flow between the basement, the upstairs, and the outdoors, although the number of zones modeled can be easily changed into an input parameter. The model also contains radon sources and sinks; therefore, the total amount of radon in the system can change over the course of time (unlike the system used to derive airflows from MTMS emissions data, where the amount of air in each zone and in the system remains constant). Outdoor air is a radon sink; the model assumes that it can absorb all the radon coming out of the house and still maintain a negligible radon concentration. The soil gas around the basement is the only radon source.

Figure 6 shows the connections between the different compartments of an extended radon model, and how each compartment can draw from either measured or modeled data to produce input for the next compartment. The effects of weather, temperature differences, and the use of air distribution systems on pressure differences is the first compartment of the model. These parameters can either be modeled themselves in simulations of the effect of these parameters on radon entry, or input as measured time series. The resulting pressure

differences can be used to model airflows. Alternatively, pressure differences can be measured directly and used to predict airflows. Difficulties in predicting airflows from pressure differences are discussed in Appendix A of this report. Alternatively, one can measure airflows directly using tracer gases. The airflows can then be used with either a measured or modeled radon entry rate to circulate the radon between the basement and the upstairs.

The flow model presented here takes as input the measured flows between zones and the infiltration from outdoors every half-hour (a convenient time period), the initial radon concentrations in both zones, and an average entry rate into the basement. The model assumes the flows are constant over each half-hour period and that the radon entry rate is constant over the whole simulation period. The assumption of a constant entry rate is strong and somewhat inaccurate, as seen by the time variations in entry rate shown in Figure 7. The assumption is used for the sake of simplicity, and we will discuss the associated error in more detail below. The model predicts the radon concentrations in each zone for each half-hour by iterating the following set of equations over short periods of time during which the radon concentrations in each zone are held constant (we have used 1 minute in this analysis, but we have also found that the whole-period average and the RMS error are not highly sensitive to iteration frequencies between 1 and 30 minutes).

$$[Rn(t)]_i \text{ (predicted)} = [Rn(t-1)]_i + [Rn(t)]_i\text{(inflow)} - [Rn(t)]_i\text{(outflow)}$$

where

$$[Rn(t)]_i \text{ (inflow)} = \frac{\Delta t}{vol_i} x \left[\sum_j F(t-1)_{j \rightarrow i} x [Rn(t-1)]_j + \dot{Rn} \right]$$

$$[Rn(t)]_i \text{ (outflow)} = [Rn(t-1)]_i x \frac{\Delta t}{vol_i} \sum_j F(t-1)_{i \rightarrow j}$$

and where

i,j	index the different zones--basement, upstairs, and outdoors in this model;
$F(t)_{i \rightarrow j}$	is the flow from zone i to zone j during the time period from t-1 to t, in this case measured with the MTMS system;
$[Rn(t)]_i$	represents the radon concentration in zone i at time t;
vol_i	is the volume of zone i;
Δt	is the short time period during which radon concentrations in each zone are held constant; and
Rn	represents a radon entry rate from outdoors, which is 0 except in the basement.

These equations neglect radon decay, which is very much smaller than the included terms. The inflow and outflow terms are on the order of 100 to 1000 pCi/L, while the decay term would be on the order of 1 pCi/L. The inflow and outflow terms are not actual measured

concentrations; they are radon flows into or out of a zone, scaled by the zone volume to determine how they will change the radon concentration in that zone.

Figure 8 shows the output of the model. The top plot compares measured and simulated radon concentrations in the basement while the bottom plot compares the measured and simulated concentrations upstairs, both for the 1-week MTMS flow measurement period. This simulation used soil radon entry rates calculated from the MTMS emissions data (see above, section II), 31 μCi/hr for the initial EH day and 37 μCi/hr thereafter. The general behavior of the modeled basement radon matches the measured radon fairly well; sudden peaks and drops in the measured radon concentration also appear in the modeled radon level. The simulated concentration varies more than the measured concentration, with higher peaks and lower troughs. The overall simulated average is slightly too high in the basement and slightly too low upstairs, predicting 287 pCi/L in the basement and 69 pCi/L upstairs as opposed to average measured values of 277 and 89 pCi/L, respectively. For the basement, the error of the average falls roughly within the 2% to 10% error of the flows. The RMS errors of 60 pCi/L for the basement concentration and 25 pCi/L for the upstairs during GC are somewhat greater, at about 25% of the average levels. On the whole, however, the flow model predicts the average radon concentration quite well and the fine-scale behavior of radon reasonably well--especially given the assumption of a constant entry rate. Note that the model takes the measured radon concentration as input only once, at the beginning of the run; all radon concentrations are predicted beginning from the modeled concentrations of the previous time period. The relative success of the model in predicting radon concentrations indicates that the flow measurements are accurate, and that the model itself uses reasonable assumptions.

We have also modified the flow model to check the entry rates calculated from the MTMS emissions data. Instead of using the above equations iteratively to predict radon concentrations, the modified model takes the net predicted change in basement radon concentration, not including entry from the soil, and compares it to the change in measured radon over a half-hour period. Any shortfall in radon must be made up by entry from the soil, giving an entry rate for the period. (This analysis necessarily holds radon concentrations constant over the half-hour period, but the RMS error of the unmodified flow model discussed above increases only from 60 to 67 pCi/L when one makes this assumption by changing Δt from 1 minute to 30 minutes. Holding radon constant over 30 minutes, therefore, should not add too much error to the entry rate analysis.)

Figure 7 compares this modeled entry rate to the entry rate calculated from MTMS emissions data. Once again, the modeled and actual behaviors are very similar. The averages, 36.2 μCi/hr from the model and 36.7 μCi/hr from the emissions data, are again well within the experimental error of the flows, although the RMS error of 10.5 μCi/hr is high. The success of the model in matching the entry rates

calculated in a different way provides a reassuring check of the validity of the assumptions used, both in constructing the model and in reducing the emissions data to airflow data. We could now reconstruct radon entry rates with some confidence from a set of interzone airflow and radon concentration measurements, without going back to raw emissions data which relate the tracer gas emission rate and concentration in the basement to the radon entry rate and concentration (as explained in section II). The flow model can estimate radon entry rates given radon concentrations and any set of airflow data, whether measured with tracer gas techniques or estimated in another way.

V. HAC INTERACTION

HAC and radon entry. Use of a heating or air conditioning unit located in a basement or crawlspace which distributes conditioned air via an air handler system (HAC), such as the gas combustion unit described above, can have a variety of effects on radon entry before mitigation. These effects have been discussed in the preceding sections in detail for one research house. In general, pre-mitigation effects include depressurization of the substructure due to two different mechanisms. First, combustion of the fuel itself results in loss of air in the basement due to the combustion and increased stack losses out the furnace chimney. For example, in the research house discussed in the preceeding sections, Princeton house #21, the flow out the basement flue was 60 m^3/hr when the flue was cold due to stack flow alone and 100m^3/hr during gas combustion. Second, use of the air handler can take more air from the basement than it returns because of leaky return ducts. This happens because the return ducts are depressurized relative to the basement, and if they are leaky they will pull basement air into them. Also, supply and return duct systems are often imbalanced, and often the imbalance occurs because there are more supply ducts to the upstairs from the basement than there are returns to the basement from the upstairs. Thus, the basement is depressurized since more air is pulled out of the basement than is returned. These effects will vary between houses and are completely house dependent. Basement pressurization is also possible when supply ducts are leakier than returns, although we have not observed HAC pressurization in any of our research houses. Diagnostic measurements can determine which mechanisms are dominant in a particular house. The diagnostic protocol developed at Princeton includes the diagnostic measurements which we feel are most useful(9).

HAC and subslab depressurization mitigation. The HAC system can also have an influence on the efficient operation of a subslab depressurization (SSD) system. Recall that SSD mitigation works by depressurizing the subslab air relative to the basement air, so that air is no longer pressure-driven from the subslab to the basement air. If an SSD system is working with only a slight pressure difference between the basement and the subslab, then the HAC system may possibly overpower the SSD system when it comes on. That is, when the HAC system starts, the added depressurization which it causes in the basement could be enough to overcome the depressurization established by the SSD

system. Figure 9 illustrates this interaction with a subslab depressurization system. It shows, in the top box, the radon concentration in the basement in PU/ORNL Piedmont House 6. (The substructure configuration and the mitigation system is described in reference 2.) The bottom box shows the percent of each half hour the HAC and air handler is on. House 6 had a subslab depressurization system installed and running at full capacity when this data was recorded. There were areas under the slab or in the hollow block walls where the depressurization due to the SSD system was slight enough to be overcome by the air handler. When the air handler ran the pressure field again favored flow of soil gas indoors, and the radon levels rose. HAC use explains 32% of the variation in the basement radon during the six days shown in Figure 9. This correlation is not overwhelming, but it is not much worse than typical correlation coefficients for this kind of analysis. In the absence of more detailed statistical analysis, and in combination with the clear pattern shown in Figure 9, it indicates a clear interaction between the HAC system and the SSD mitigation system.

HAC and the flow model. The effects of the HAC system are not explicitly incorporated in the flow model. Instead, the HAC influence on the radon concentrations appears implicitly in the measured flows, which change in response to the pressure differences created by the operation of the HAC system, as displayed in Figure 1. The HAC system forces air from basement to upstairs with its air handler fan, allows some air to come back to the basement via return ducts, and changes the pressure balance within the house to create other flows. The current model is set up to use measured flows as input. But these flows could also be modeled, as we discussed with regard to Figure 6. Modeling the airflows associated with the increased pressure differences across the basement (or substructure) boundaries requires some knowledge of the leakiness across each boundary, or some other way of parameterizing the relationship between the flow and pressure differences. Pressure-flow relationships are discussed more fully in Appendix A of this report.

VI. CONCLUSION

This report has presented the distinct differences in radon and airflow behavior characteristic of two heating systems running in the same house. This comparison is particularly useful, because it allows an analysis of the effects of the heating systems while holding the other characteristics of the house constant. Radon distribution within the house, radon entry rate, and flows around the house have different behaviors under each heating system. This information is useful both on a practical level, in assessing radon concentrations and health risks in houses with different heating systems, and on a more scientific level, for understanding the characteristics of radon flow and general airflow in houses.

Along with the specific information about house dynamics, this report has also introduced a number of analysis and modeling

techniques. In particular, we have made preliminary attempts at deducing airflow and radon behavior around the house substructure. This behavior is very difficult to measure directly, and it is our hope that the flow model presented here will help to illuminate this behavior and check other results, as well as being the first step toward a more extensive macroscopic model of the movement of radon in and around houses.

VII. REFERENCES

1. Matthews, T.G., Hubbard, L.M., Dudney, C.S., Socolow, R.H., Hawthorne, A.R., Gadsby, K.J., Harrje, D.T., Bohac, D.L., Wilson, D.L., "Investigation of Radon Entry and Effectiveness of Mitigation Measures in Seven Houses in New Jersey," mid-project report, ORNL/TM-10671, June, 1988.

2. Dudney, C.S., Hubbard, L.M., Matthews, T.G., Socolow, R.H., Hawthorne, A.R., Gadsby, K.J., Harrje, D.T., Bohac, D.L., Wilson, D.L., "Investigation of Radon Entry and Effectiveness of Mitigation Measures in Seven Houses in New Jersey," Final report (draft), ORNL-6487, September, 1988.

3. Dickerhoff, Darryl, Sherman, Max, Amarel, I., "Technical Description of the Multigas Measurement System," in preparation.

4. Sherman, Max, "On Estimation of Multizone Ventilation Rates from Tracer Gas Measurements," (Draft, LBL-25772).

5. Dickerhoff, Darryl, personal communication, September, 1988.

6. Hubbard, L.M., Gadsby, K.J., Bohac, D.L., Lovell, A.M., Harrje, D.T., Socolow, R.H., Matthews, T.G., Sanchez, D.C., "Radon Entry into Detached Dwellings: House Dynamics and Mitigation Techniques," accepted by Radiation Protection Dosimetry, 1988.

7. Hubbard, L.M., Bohac, D.L., Gadsby, K.J., Harrje, D.T., Lovell, A.M., Socolow, R.H., "Research on Radon Movement in Buildings in Pursuit of Optimal Mitigation," Proceedings of the ACEEE 1988 Summer Study on Energy Efficiency in Buildings, Asilomar, CA, 1988.

8. Hubbard, L.M., Bolker, B.M., Hull, D.A., Gadsby, K.J., Harrje, D.T., and Socolow, R.H. Princeton CEES final report for DOE, Section III, December, 1988.

9. Gadsby, K.J., Hubbard, L.M., Harrje, D.T., Rapid Diagnostics, presented at and to appear in the proceedings of the EPA Radon and Radon Reduction Technology Conference, Denver, Colorado, Oct. 1988 (paper VI-P1).

Table 1. Heating periods at House PU21: averaged measured quantities.

	electric heat	gas combustion/ automatic setback
Julian days	74.8-75.8 [45-55]*	75.7-83 [37-44]
Zone volumes: (m^3)		
basement	118.5	
upstairs	467.1	
Radon concentration: (pCi/L)†		
[Rn], basement	[302] 362	[245] 265
[Rn], upstairs	[51] 48	[112] 95
[Rn], subslab	[1460] 1505	[2077] 2081
[Rn], whole house (volume-weighted average)	[102] 114	[139] 132
Pressure differences: (Pa)		
outdoors-basement	[2.19] 1.72	[3.39] 2.48
subslab-basement	[1.80] 1.46	[2.60] 1.91
upstairs-basement	[0.16] 0.01	[0.85] 0.53
HAC system use: (percent on)	0	[34.7] 22.4
Entry Rate: (μCi/hr)		
from MTMS data	31,9	37.4
Flows: (m^3/hr(ACH))		
Infiltration-		
basement	67(0.57)	93(0.78)
upstairs	132(0.28)	147(0.31)
basement to upstairs	10	80
upstairs to basement	33	87
Temperature: (^oC)		
basement	[14.9] 15.8	[20.9] 18.8
upstairs	[17.8] 17.4	[18.6] 18.1
outdoors	[1.54] 3.9	[-2.0] 2.5

* Days in brackets ([]) are alternate periods from which more data were available; quantities in brackets are taken from these periods.

† 1 pCi/L = 37 Bq/m^3

APPENDIX A. PRESSURE VERSUS FLOW CALCULATIONS

One of the blind alleys we found during our initial stage of physical modeling was our attempt to relate single measured pressure differential across each zone boundary to measured airflows between zones. The analysis is not definitively a blind alley, but we did run into a number of problems in this seemingly straightforward analysis and we may not have the time to work them out.

I. MOTIVATION

We have several reasons for wanting to know the relation between airflows and pressure differences. First, the ultimate goal of our physical modeling effort is to string together several models which focus on different steps in the entry, movement, and decay to progeny of indoor radon (see Figure 6). Starting from weather and indoor air distribution data, we would like to model pressure differences. Given a good relation between pressure differences and airflows, we could then model airflows. Finally, we could take the modeled airflows along with subslab characteristics related to radon entry and use our existing flow model (1), discussed in Section IV, to predict radon concentrations.

Relating measured pressure differences and airflows would fill in the middle link in this chain. The physical mechanisms of stack effect, wind-induced pressurization and depressurization, and pressure changes caused by mechanical ventilation are conceptually simple and well studied, and the pressure differences created by these mechanisms should not be too difficult to incorporate in a model. It would then be possible to put together the existing flow model, the pressure-flow relationship, and a model incorporating the various pressurization mechanisms to get a model which takes house characteristics and time-varying weather data as input and models radon concentrations.

Second, and more immediately, a reasonably simple relationship between pressure differentials and airflows, even to within 50%, would be a first step toward moving from measured to modeled airflows. Pressure differentials are much easier to measure than airflows. We have extremely limited time-varying airflow data in three houses, and readily useful airflow data in only one. Pressure differential measurements, on the other hand, are a standard part of our measurement protocol; we measure them in every research house. We would like to obtain a reasonably reliable predictor of airflows, in the houses for which we have simultaneous pressure and airflow data. We could use measured airflow data to check the airflows predicted from pressure differentials, assuming of course that the same data were not used to find the predictive equation. If no other procedure is found for predicting airflows from pressure differentials than actually using the measured airflows in some type of statistical fit to estimate the leakiness between zones, we may be able to use this procedure as a very rough predictor for other houses based on our guesses at the relative leakiness of the zone boundaries.

II. THEORY

The theory behind the pressure-flow relationship is conceptually simple, but difficult to apply to buildings because of the variety and complexity of airflow paths between building zones. Pressure-driven flow is theoretically explained in the extreme cases of laminar flow and turbulent flow. Real flow into and out of building zones lies somewhere inbetween, and is governed by the equation $Q = k * \Delta P^n$, where k is a leakiness coefficient (in $area^{-1} * Pascals^{-n}$) and n is a (unitless) flow coefficient that describes the nature of the flow. It falls somewhere between 0.5 (for purely turbulent flow) and 1.0 (for purely laminar flow). Tests in houses have shown that bulk flow coefficients for houses are generally around 0.65 (2). Our basic goal is to find k and n for each interzone boundary.

A model developed at Lawrence Berkeley Laboratory (3) provides another way of modeling k and n, referred to (with slight differences in definition) as "effective leakage areas" (ELAs). The LBL model relies on laboratory tests of the leakage characteristics of various materials. The derived coefficients (in ELA/length or ELA/area) are applied to the dimensions of various leakage sites, for example weatherstripped door frames or double-hung windows, and the ELAs for all the specific leakage sites are summed to derive a bulk ELA for the building.

III. DATA

We use pressure differential measurements and airflow measurements to do the analysis. Setra brand variable capacitance differential pressure transducers measure the differential pressures between the basement and subslab, upstairs, and outside, with the basement as a reference pressure. The transducers measure pressure differences at only one point across each zone boundary, although in some cases several points join in a manifold to get an average pressure difference. For example, in the Piedmont data set the outside-basement pressure transducers have a pressure tube connected to the outdoors on each side of the basement wall and manifolded to the input to the pressure transducer. This procedure gives a pressure difference between the basement and outdoors averaged over all sides of the house. Pressure differences are recorded by the data logger every 6 seconds, but the system internally averages them to half-hour points. The pressure transducers have an estimated accuracy and an estimated precision of 10% (4). The transducers also experience some zero drift, which we attempt to track by periodically checking and recording the transducer zeros and modifying our calibration constants accordingly.

Our best airflow measurements come from the Multiple Tracer Mass Spectrometer system, owned by Lawrence Berkeley Laboratory (3). This instrument gives us interzone flows each 20-minute to 1-hour period, with an associated error of about 10%. Most of our analysis on the pressure-flow relationship has used one week's worth of MTMS data taken at Princeton research house 21. We focused on a day or two of that data when the heating and air handling system (HAC) was off, to avoid the added complication of mechanical ventilation (see below, section V).

Although it does not measure interzone flows, the Constant Concentration Tracer Gas (CCTG) system should provide reasonable time-varying infiltration data which can be used in the analysis. We should at least be able to get correlations between basement-outside and upstairs-outside pressures and the relevant flows. Unfortunately, CCTG data is relatively scarce and needs a fair amount of screening to sort out unreliable data and convert to a useful format. We could do this work, but it seemed to be more profitable to spend our time on the more accessible MTMS data. In addition, the problems of mechanical ventilation (and open windows) also plagued the CCTG data.

Our third tracer gas system, the Perfluorocarbon Tracer (PFT) system, gives interzone flows but only in weekly average periods or so. Although they are useful for other analyses, these data give impressionistic answers at best for the pressure-flow relation.

IV. PROCEDURES.

We use various forms of linear regression to try to find k, n, or both at once. The actual process of looking for correlations is time-consuming, but straightforward. First, take all the pressure data: outside-basement, upstairs-basement, and the upstairs-outside pressure (the difference of the first two differential pressures). Subslab-basement pressure will also be useful for the analysis once we understand how to relate it to subslab→basement flow. Then, use all the airflows to regress relevant pressures against airflows with pressures as the independent variables: for example, ΔP out-basement vs flow out→basement and basement→out. We generally start by looking at linear fits, for simplicity. There are a number of ways to get fancier. (We have done some work with each of these techniques; none, so far, has been any great improvement over simple linear fits, but we may not have looked far enough.) The simplest is to assume an n of 0.65, raise ΔP to the nth power, and see if it improves the regression. "Power finder" routines, which step through a number of possible flow exponents (say 0.5 to 1.0 by intervals of 0.1) and give an r^2 or t-statistic for a pressure-flow regression at each value of n, can help find the best value of n. Another option is to regress (log ΔP) against (log flow), in which case k will be the intercept and n the slope of the regression line. Practically, several of these techniques are real nuisances because of the tendency of the pressures to fluctuate negative. One can probably deal with this by using $-\ln(-x)$ instead of $\ln(x)$ when x is negative, but it is a nuisance.

V. RESULTS and DIFFICULTIES.

Results from this analysis have not been very encouraging, although we admittedly haven't exhausted the possibilities. For example, ΔP out-basement vs flow out→basement has an r^2 of 0.24 using a straight linear fit.

Some of the more specific problems:

1) Regardless of the actual values of the pressure differentials, there is always some mixing back and forth between zones. One could excuse this by saying that half-hour averages mask fluctuation between positive and

negative differential pressures between two zones. Even if the half-hour pressure average is decidedly positive, however (in which case the pressure gradient should always be in the same direction and theory would say that the flow could only go in the direction towards lower pressures), there is some flow in each direction. We tried for a while to come up with "mixing numbers," to see if the backflow, the flow against the nominal pressure gradient, was proportional to the flow with the gradient. It didn't feel, however, that we were getting at anything of physical significance this way. Another way to deal with this is to try fitting to net flow. Even if this is successful, however, it may not provide the detailed airflows needed to model mixing of radon between zones. The underlying problem seems to be the spatial and temporal variability of pressure differences and leakiness.

We can try to write off the temporal variability by saying that a highly positive average pressure difference must mean the pressure was in the same direction for the entire averaging period, but we have no good way of dealing with the spatial variability. A different pressure and a different leakiness at a point a few meters away from the measurement point may produce a different flow path that behaves quite differently. We can do a bit of guesswork to account for major flow paths (see (2) below) but we cannot really deal with many small, randomly pressurized flow paths. It may be that a detailed analysis of different flow paths is really required to model airflows, in which case this analysis will be too coarse to work. Conventional wisdom assumes homogenous leakiness across a house boundary; no-one in the research community seems to have the data to say just how gross the assumption is. (We hope for some light from a senior thesis in progress by a Princeton senior which will do detailed measurements of the pressure profile of a building envelope.)

2) Other major flow paths, as mentioned above, can foul things up. In Princeton house 21, where we have done most of this analysis, we know from other measurements that a flue accounts for 60 m^3/hr of airflow from the basement to the outside, even when it is completely cold. Clearly, the flue has different coefficients k and n and probably its own stack pressure driving flow through it. This case is a beautiful example of how other flow paths can confound the analysis which assumes that all flow can be lumped together in a bulk $Q = k\Delta P^n$ equation. One can account for the flue flow by simply subtracting 60 m^3/hr from the outside→basement flow and correlating the rest of the flow with outside-basement pressure, but the point is that one doesn't always know about the other flow paths, or know the flow through them quantitatively.

3) Another indication of the spatial variability of flows and pressures is the disturbing case where all of the net pressures measured would seem to force air into the basement. This inflow would eventually make the basement explode. Most airflow analysis includes a mass balance equation, which automatically deals with this problem; our analysis just uses measured pressures. What the problem tells us is that there must be other points at which the pressure gradient is reversed and air is able to flow out of the basement, such as out flues or duct systems.

4) Interference from forced-air ventilation systems is theoretically simple, but practically difficult to correct. When the forced-air system comes on the basic assumption of simple pressure-driven flow no longer works. In most cases we do have independent measurements of HAC use, so we might be able to calculate the amount of airflow caused by the HAC system and ignore it in the analysis. Unfortunately, HAC use also causes pressure changes which complicate the process of removing the HAC contribution to airflow. The proper way to remove HAC contributions is to measure the flows in the HAC system when the system is on, and then subtract these flows (scaled by the amount of time the HAC system was running in a given half-hour) from the measured flows to get purely pressure-driven flow. We have not yet been able to get flow measurements in the HAC system in our houses. Therefore, all of the CCTG data and all but a few days of the MTMS data are useless for the analysis; the pressure-driven flow component in the data is overwhelmed by the forced-air flows created by the HAC system.

5) Another problem, which we have also had to deal with in our budget calculations (see Appendix B), is the unknown contribution of soil gas to airflows into the basement. Outside→basement flow as we define it includes flow from the soil gas. In many cases the subslab-basement pressure seems to be a good predictor of outside→basement flow. How can we best combine the outside-basement and subslab-basement pressure differentials to predict outside→basement flow? Clearly neither is correct by itself, and we may have a chance to get around some of the spatial variability problem by including another pressure measurement, but we don't really know how to proceed. As you may have guessed, this problem is yet another manifestation of our problem with spatial variability of pressures and flows.

6) Finally, a small technical anomaly which we haven't figured out yet. When we apply the power finder (see (IV) above) to the data, we sometimes get very odd results for an optimum flow coefficient. The regression coefficients seem better at n=1 than they are at n=0.5, but they are also better at n=2 than at n=1. This phenomenon is probably just a function of statistical noise, since the r^2 were very poor and got only slightly better.

All of our problems basically come back to spatial and temporal variability of pressure measurements. $Q = k * \Delta P^n$ holds for one point or airflow path in a basement at one moment in time; our problem is how much we can aggregate this relationship and still get good correlations. We think we can sweep temporal variability at least partway under the rug, but spatial variability is popping up in many different ways. A slightly more intensive effort on the data using the same old statistical techniques more thoroughly should show once and for all whether the approach will work. More field experiments on pressure and flow variability may say whether there are other ways around the problems.

VI. REFERENCES

(1) Hubbard, L.M., Bolker, B.M., Socolow, R.H., Dickerhoff, D., Mosley, R.B., "Radon Dynamics in a House Heated Alternately by Forced Air and by Electric Resistance," presented at and in the Proceedings of the USEPA

1988 Symposium on Radon and Radon Reduction Technology, October 18-21, 1988, Denver, Colorado.

(2) Sherman, M.H., Wilson, D.J., and Kiel, D.E., "Variability in Residential Air Leakage," in Measured Air Leakage of Buildings, ASTM STP 904, pp. 349-364 (Philadelphia, 1986).

(3) Sonderreger, R., and Reinhold, C., Component Leakage Areas in Residential Buildings, Lawrence Berkeley Laboratory (LBL-16221), 1983.

(4) 1987 Piedmont project QA/QC document, Section 5, p. 3.

(5) Dickerhoff, Darryl, Sherman, Max, Amarel, I., "Technical Description of the Multigas Measurement System," in preparation.

VII. MODELING REFERENCES

Axley, James, "Progress toward a general analytical model for predicting indoor air pollution in buildings," Indoor Air Quality Modeling Phase III report, publication #NBSIR88-3814 (July, 1988), National Bureau of Standards.

Camp Dresser & McKee Inc., Model Development and Formulation for the New Jersey Statewide Scientific Study for Radon, Task 2 Final Report, Edison, NJ (December 1987).

D'Ottavio, T.W., and Dietz, R.N., "Radon transport into a detached one-story house with a basement: Discussions," Atmospheric Environment, 20:5:1065-1067, 1986.

Hubbard, L.M., Bolker, B.M., Socolow, R.H., Dickerhoff, D., Mosley, R.B., "Radon Dynamics in a House Heated Alternately by Forced Air and by Electric Resistance," presented at and in the Proceedings of the USEPA 1988 Symposium on Radon and Radon Reduction Technology, October 18-21, 1988, Denver, Colorado.

Kokotti, H., Kalliokoski, P., Raunemaa, T., "Analysis of Indoor Radon in Different Ventilation Systems," presented at and in the Proceedings of the USEPA 1988 Symposium on Radon and Radon Reduction Technology, October 18-21, 1988, Denver, Colorado.

Liddament, M.W., Air Infiltration Calculation Techniques--An Applications Guide, Air Infiltration and Ventilation Centre, Bracknell, Great Britain, 1986.

Mowris, R.J., "Analytical and Numerical Models for Estimating the Effect of Exhaust Ventilation on Radon Entry in Houses with Basements or Crawl Spaces," M.S. Thesis (University of Colorado), Lawrence Berkeley Laboratory, LBL-22067, August, 1986.

Mowris, R.J., and Fisk, W.J., "Modeling the Effects of Exhaust Ventilation on ^{222}Rn Entry Rates and Indoor ^{222}Rn Concentrations," Health Physics vol. 54, No. 5 (May, 1988), pp. 491-501.

Nazaroff, W.W., Feustel, H., Nero, A.V., Revzan, K.L., Grimsrud, D.T., Essling, M.A., and Toohey, R.E., "Radon transport into a detached one-story house with a basement," Atmospheric Environment, 19:1:31-46, 1985.

Sherman, M.H., and Grimsrud, D.T., "Measurement of infiltration using fan pressurization and weather data," in 1st AIC Conference, "Air infiltration instrumentation and measurement techniques," Proceedings, 1980, U.K.

Sonderreger, R., and Reinhold, C., Component Leakage Areas in Residential Buildings, Lawrence Berkeley Laboratory (LBL-16221), 1983.

Qingyan, Chen, Indoor Airflow, Air Quality and Energy Consumption of Buildings, Ph.D thesis, Technical University of Delft (1988), ISBN 90-9002435-2.

APPENDIX B. BUDGET CALCULATIONS: AIRFLOW AND RADON ENTRY

The idea of budget calculations for either airflow or radon entry is to take a bulk infiltration or radon entry rate and try, by applying various pieces of information from either measurement or models, to disaggregate it into flows from more specific places. Ideally, one should be able to break down infiltration into an airflow budget, multiply each of the specific airflows by the radon concentration in its area of origin, and sum these radon entry rates to regain the bulk radon entry rate originally calculated or measured some other way. If we could achieve this goal, we would learn more about the importance of specific radon entry routes and thus about radon control. Some possibilities for obtaining bulk radon entry rates are: use tracer gas emissions data and radon concentrations (1); use airflow data and radon concentrations in the flow model (2); ventilate the area, close it up, and estimate entry rate from the ingrowth rate. The first two methods can give either time-varying or integrated measurements, depending on the time scale of the tracer gas measurements or of the flow model. The last procedure gives a radon entry rate at one point in time.

In practice it doesn't seem to work. Airflow budgets present many problems. For example, estimating the leakiness of various parts of the room, the band joist in particular, is a matter of guesswork within broadly defined bounds; we also use an average number for block wall leakinesses which are known to vary from house to house and wall to wall. Also, pressure differentials, which are needed to determine airflow, are often measured across only one point on a boundary surface and taken to be representative of an entire interface. Our procedure for estimating flow through the floor/wall crack is suspect; it assumes soil of homogenous permeability surrounding the basement, which is certainly untrue when there is a subslab gravel bed, and which may change the results substantially.

The accuracy of the radon budgets are dependent on the airflow budgets, with all their uncertainties, but have their own particular problems as well. The spatial variability of radon concentrations means that our disaggregation of the radon entry routes at the level of block walls, floor/wall crack, and band joist may still be too coarse. When radon concentrations can vary by an order of magnitude under a slab, multiplying an average subslab-basement airflow by an average subslab radon concentration becomes dubious.

The final fate of budget calculations depends on where the greatest source of error lies. If the basic problem is with assumptions which cannot easily be replaced with more sophisticated ones, or if the problems of spatial variability cannot be overcome by some reasonable averaging scheme, then budgets are basically unworkable. If, on the other hand, a few more measurements or a more thorough approach to the estimates will make a budget work, then this approach may be useful.

Our approach. We looked at the floor/wall crack, the hollow block walls, and the band joist as the primary flow paths for infiltration. For the floor/wall crack we used an analysis done by Mowris (see eq. 20 in reference

3), which predicts the flow through the floor/wall crack or gap as a function of crack width, soil permeability, crack length, pressure differential, and basement depth. We simply used Mowris's equation with our data to estimate this flow, incidentally coming up with small airflows (on the order of 0.05 ACH). Mowris's analysis uses a resistance network concept to combine the resistance of the soil and the resistance of the perimeter crack which is the entry point for soil gas flow into the basement. He then takes the combined resistances and says that (again using an electrical analogy) $Q = \Delta P/R_{tot}$, where Q is the flow, ΔP is the pressure difference across the flow boundary, and R_{tot} is the combined resistance.

For the hollow block walls we used an analysis by Marynowski (4) which uses the expression for flow through hollow block walls of the form $Q = k\Delta P^n$, where Q is again the flow and ΔP is again the pressure difference across the flow boundary. Marynowski's analysis gives an average coefficient for k per m^2 of wall area and an average n. The total airflow from the walls comes from the total wall area, the coefficients k and n, and the pressure differential across the wall. (It is possible that this component, which doesn't account for soil resistance in the same way as Mowris's analysis, should be used with some sort of soil resistance term to account for how much soil gas is actually availabe to flow through the walls. Actually calculating these flow paths and resistances is difficult.)

The flow through the band joist (and other outstanding flow paths; windows, etc.) comes from the standard "effective leakage area" (ELA) approach (5), where cracks and joints are given an ELA or a k-value per unit length. If ELA is given, the appropriate equation is $Q = (ELA)(2\Delta P/\rho)^{0.5}$ (where ρ is the density of air in kg/m^3; we use a value of 1.24 kg/m^3). If k is given, an accompanying flow exponent (n) is usually given as well and the same equation works as for hollow block walls.

There are a few possibilities for refining these efforts. If interzone flows have been measured, then either the "upstairs" or the "outside" (usually subslab plus area behind the walls plus above-grade area) flow can be factored out and the other flow looked at more carefully. Blower door measurements can find a bulk ELA for a basement, which might be helpful. It might also be possible to do tricky things with tracer gases.

Once the airflow budget is done, we take the resulting airflows and multiply by the various radon concentrations. We multiply floor/crack flows by subslab radon, flow through block walls by radon in the interior of the wall, flow from upstairs by upstairs concentrations, and flow from outside by zero (certainly close enough for the kind of approximations we're making). These radon flows should make up a "radon budget" which sums to the total radon entry rate, as determined (for example) by procedures described in the first paragraph.

REFERENCES FOR BUDGET CALCULATIONS

1. Hubbard, L.M., Gadsby, K.J., Bohac, D.L., Lovell, A.M., Harrje, D.T., Socolow, R.H., Matthews, T.G., Sanchez, D.C., "Radon Entry into Detached Dwellings: House Dynamics and Mitigation Techniques", accepted by Radiation Protection Dosimetry, 1988.

2. Hubbard, L.M., Bolker, B.M., Socolow, R.H., Dickerhoff, D., Mosley, R.B., "Radon Dynamics in a House Heated Alternately by Forced Air and by Electric Resistance," presented at the USEPA 1988 Symposium on Radon and Radon Reduction Technology, October 18-21, 1988, Denver, Colorado.

3. Mowris, R.J., and Fisk, W.J., "Modeling the Effects of Exhaust Ventilation on ^{222}Rn Rates and Indoor ^{222}Rn Concentrations," Health Physics Vol. 54, No. 5, pp. 491-501 (1988).

4. Marynowski, J.M., "Measurement and Reduction Methods of Cinder Block Wall Permeabilities", Princeton University/CEES Working Paper No. 99, 1988.

5. Sonderreger, R., and Reinhold, C., Component Leakage Areas in Residential Buildings, Lawrence Berkeley Laboratory (LBL-16221), 1983., and Liddament, M.W., Air Infiltration Calculation Techniques--An Applications Guide, Air Infiltration and Ventilation Centre, Bracknell, Great Britain, 1986.

FIGURE CAPTIONS.

Figure 1. Radon concentrations, pressure differentials, and HAC use in house PU21 for a gas combustion/automatic setback (GCAS) period. The top plot shows radon concentrations in the basement (solid line) and below the basement slab (dashed line), in pCi/L (1 pCi/L = 37 Bq/m^3). The bottom plot shows pressure differentials in Pascals between the basement and the outdoors (solid line) and the basement and the subslab (dashed line); basement pressure is the reference. The solid line at the bottom of the plot shows what percent of each half-hour period the HAC system was running.

Figure 2. Radon concentrations and pressure differentials in house PU21 for an electric heat period. The top plot, as in Figure 1, shows basement and subslab radon concentrations in pCi/L. The bottom plot shows only pressure differentials in Pascals; the HAC system was off during this period. High winds (10-15 mph, or 4.5-6.7 m/s) on days 53 and 54 caused the pressure spike shown on the bottom plot.

Figure 3. Radon concentrations within the basement hollow block wall (solid line), in pCi/L (1 pCi/L = 37 Bq/m^3), and HAC use (dashed line), in percent time on, at house PU21.

Figure 4. Average radon concentrations (top), in pCi/L, and pressure differences (bottom), in Pascals, during a 7-day gas combustion/autosetback (GCAS) heating period and a 10-day electric heating period in house 21. The GCAS heating period lasted from 2/5/88 to 2/12/88, during which time the air handler ran 23% of the time, while the electric heating period lasted from 2/13/88 to 2/23/88.

Figure 5. Modeled radon entry rate into the basement of house 21 (top box), in $\mu Ci/hr$, and theoretical lower and upper bounds for soil gas flow into the basement (bottom box), in m^3/hr. The radon entry rate is derived using emissions data from the MTMS tracer gas system (see text). The upper bound on soil gas flow (bottom box, dashed line) is the total flow of outside air, air originating outside all MTMS measurement zones, into the basement. Soil gas clearly makes up some but not all of this flow. The lower bound on soil gas flow (bottom box, solid line) is the radon entry rate divided by the radon concentration in the subslab, which was measured at the highest-radon point in the basement substructure. If all infiltrating soil gas came in with this maximum radon concentration, this minimum soil gas flow would bring the basement up to the measured radon concentrations.

Figure 6. Schematic diagram of a complete model for radon entry into houses. The box in the upper lefthand corner shows the zones and the directions of interzone flow which are incorporated in the model. The rest of the page shows the relationships between the various possible components of the model.

Figure 7. Radon entry rate from soil gas into the basement of house PU21 as calculated from MTMS emissions data (solid line) and from the flow model using MTMS flow data (dashed line), in $\mu Ci/hr$ (1 $\mu Ci/hr$ = 37 MBq/hr).

Figure 8. Radon concentrations in house PU21 as measured (solid line) and as simulated by the interzone flow model (dashed line), using MTMS airflow data, an estimated constant entry rate of 31 μCi/hr during electric heat and 37 μCi/hr during GCAS, and initial radon concentrations as measured at the beginning of the period. All concentrations are in pCi/L (1 pCi/L = 37 Bq/m^3). The top plot shows basement concentrations, the bottom plot shows upstairs concentrations.

Figure 9. HAC fan effects in House 6 during an early phase of mitigation, Julian days 83 to 89. The top box shows radon concentration in the basement, in pCi/L; the bottom box shows air handler use, in percent on time during each half-hour measurement period. The figure illustrates how the air handler can depressurize the basement enough partly to overcome the effects of the SSD mitigation system.

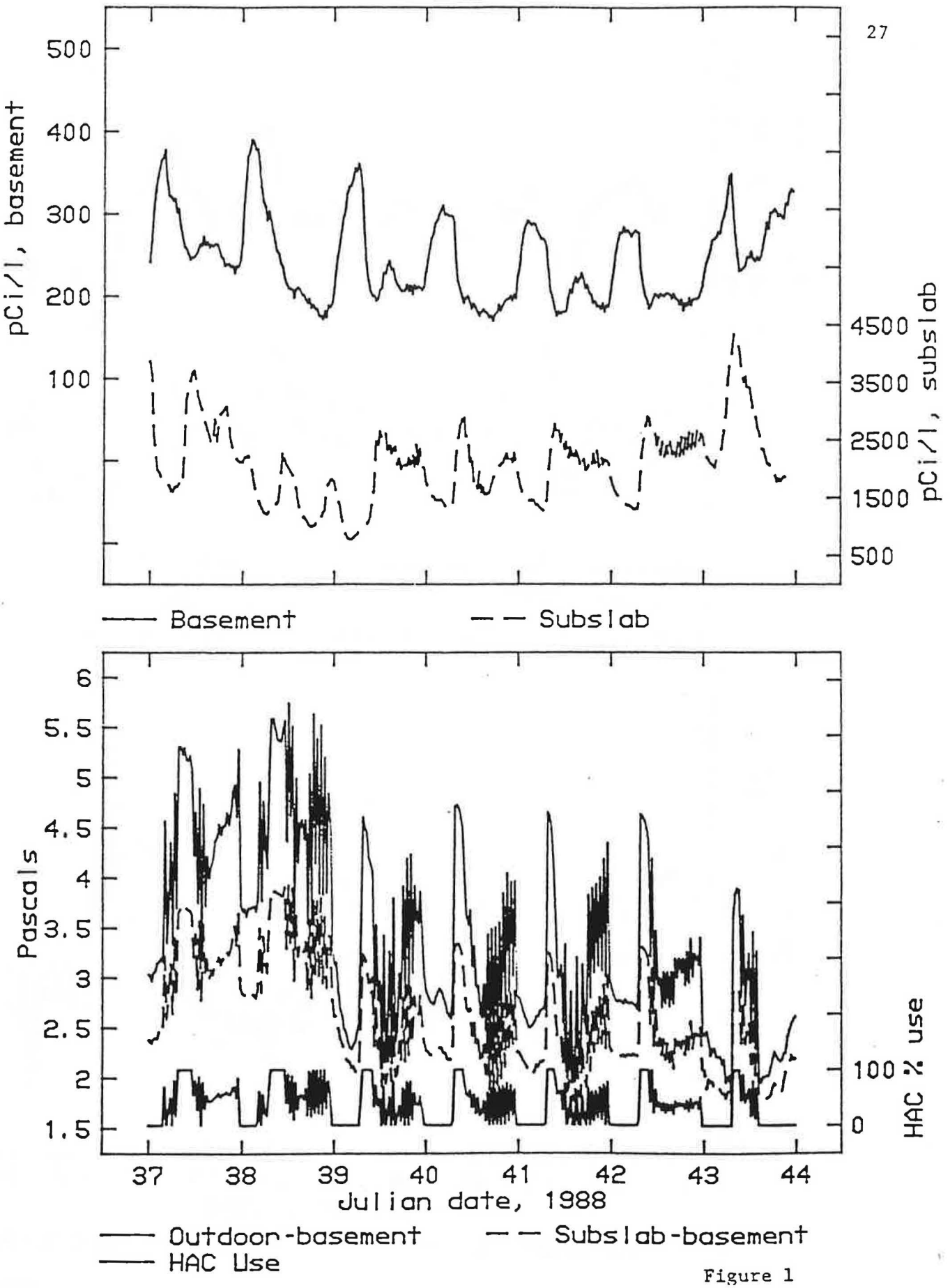
500
400
300
200
100
pCi/l, basement
4500
3500
2500
1500
500
pCi/l, subslab
Basement
Subslab
6
5.5
5
4.5
4
3.5
3
2.5
2
1.5
Pascals
100
0
HAC % use
37
38
39
40
41
42
43
44
Julian date, 1988
Outdoor-basement
Subslab-basement
HAC Use

Figure 1

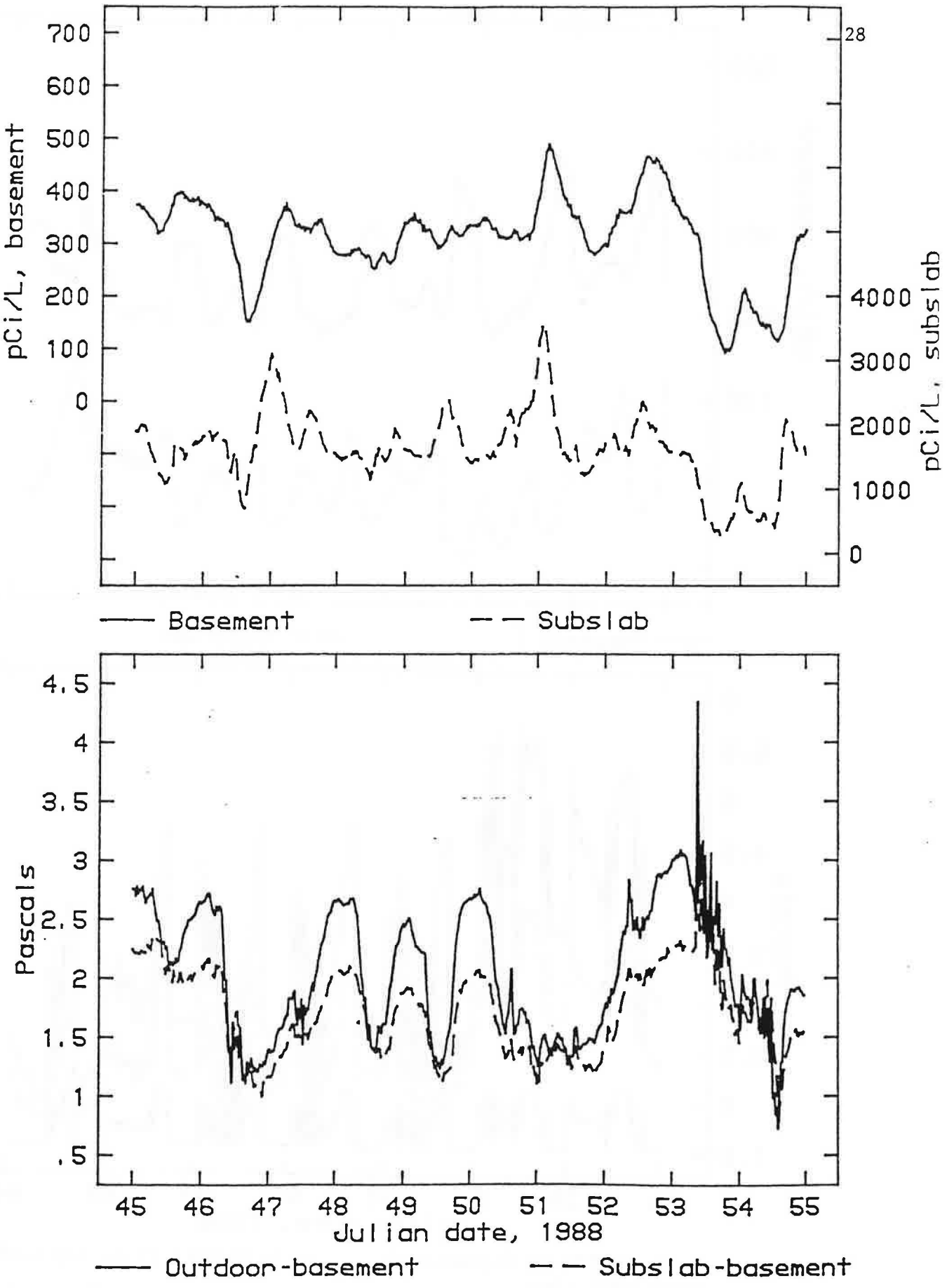
700
600
500
400
300
200
100
0
pCi/L, basement
28
4000
3000
2000
1000
0
pCi/L, subslab
Basement
Subslab
4.5
4
3.5
3
2.5
2
1.5
1
.5
Pascals
45
46
47
48
49
50
51
52
53
54
55
Julian date, 1988
Outdoor-basement
Subslab-basement

Figure 2

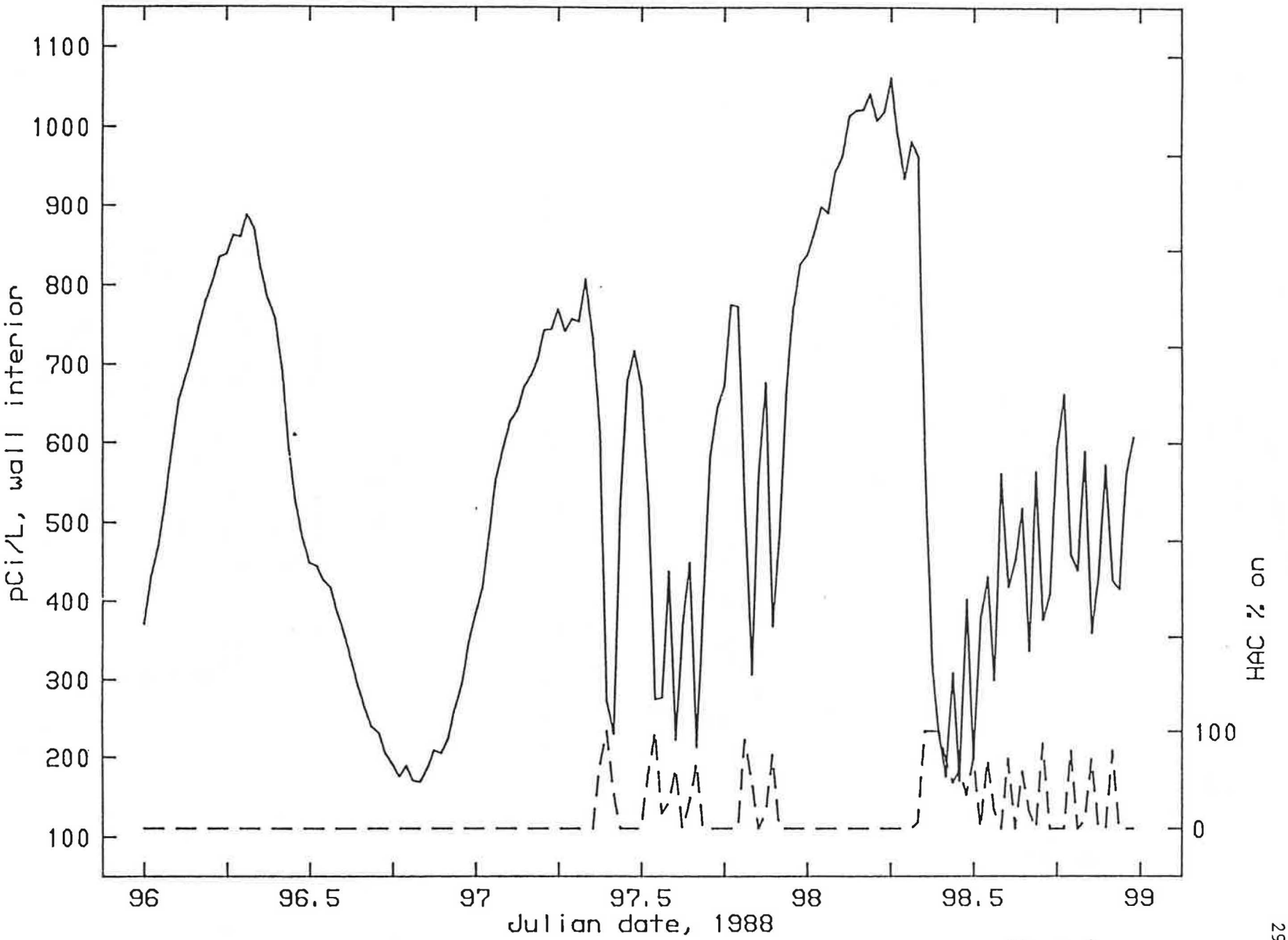
1100
1000
900
800
700
600
500
400
300
200
100
pCi/L, wall interior
96
96.5
97
97.5
98
98.5
99
Julian date, 1988
100
0
HAC % on

Figure 3

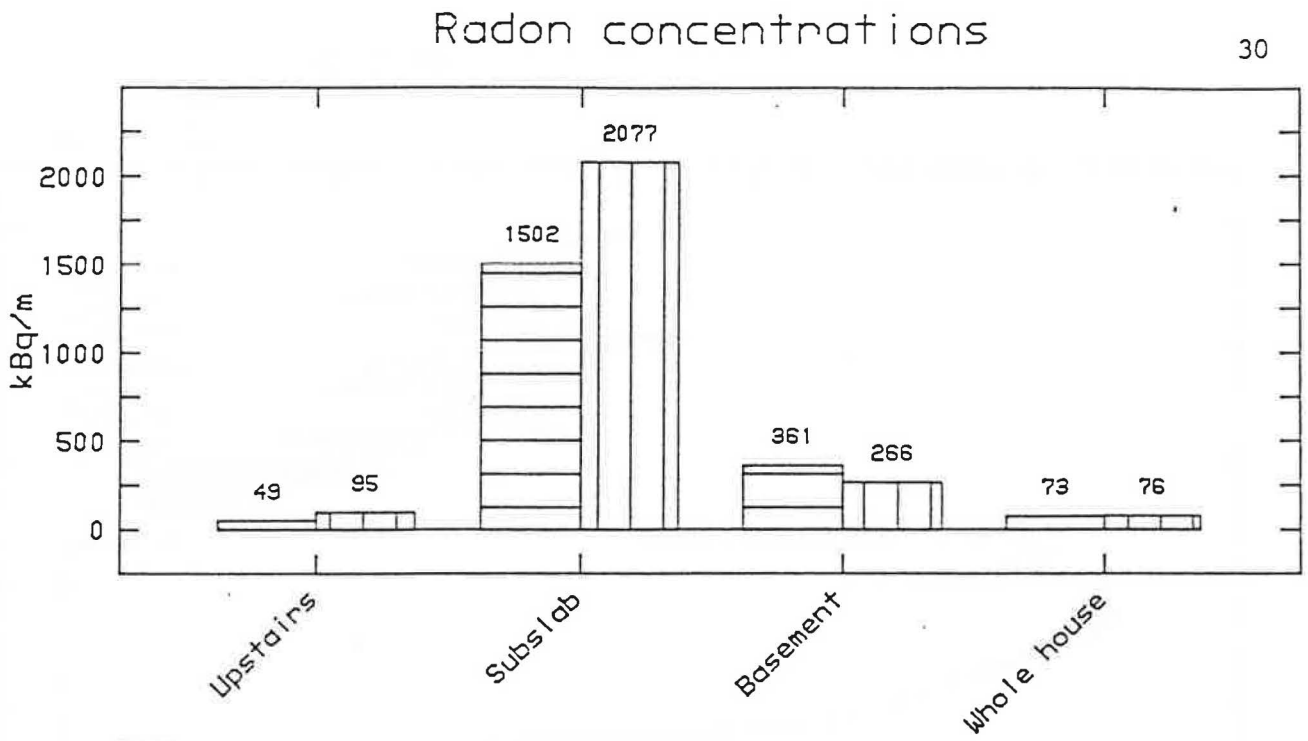
Radon concentrations
kBq/m
2000
1500
1000
500
0
49
95
1502
2077
361
266
73
76
Upstairs
Subslab
Basement
Whole house
Electric heat
Gas combustion/autosetback
Air handler ran 23% of the time
2/5/88-2/24/88

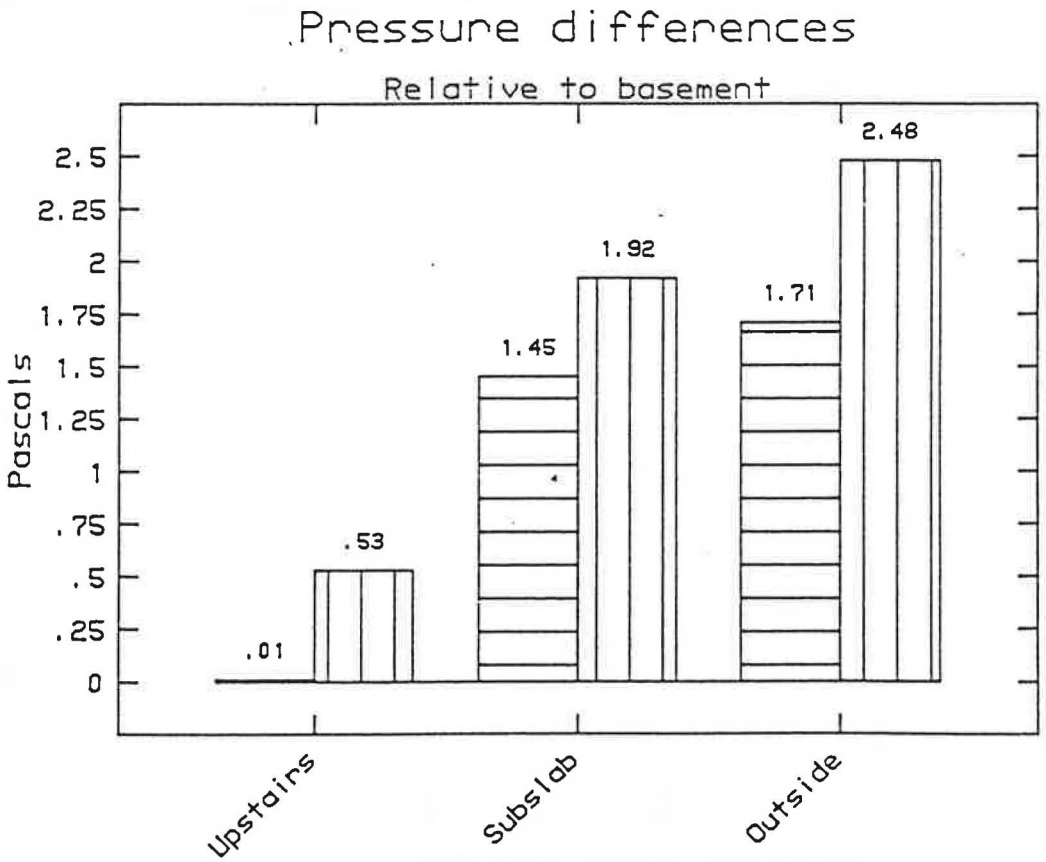
Pressure differences
Relative to basement
Pascals
2.5
2.25
2
1.75
1.5
1.25
1
.75
.5
.25
0
.01
.53
1.45
1.92
1.71
2.48
Upstairs
Subslab
Outside

Figure 4

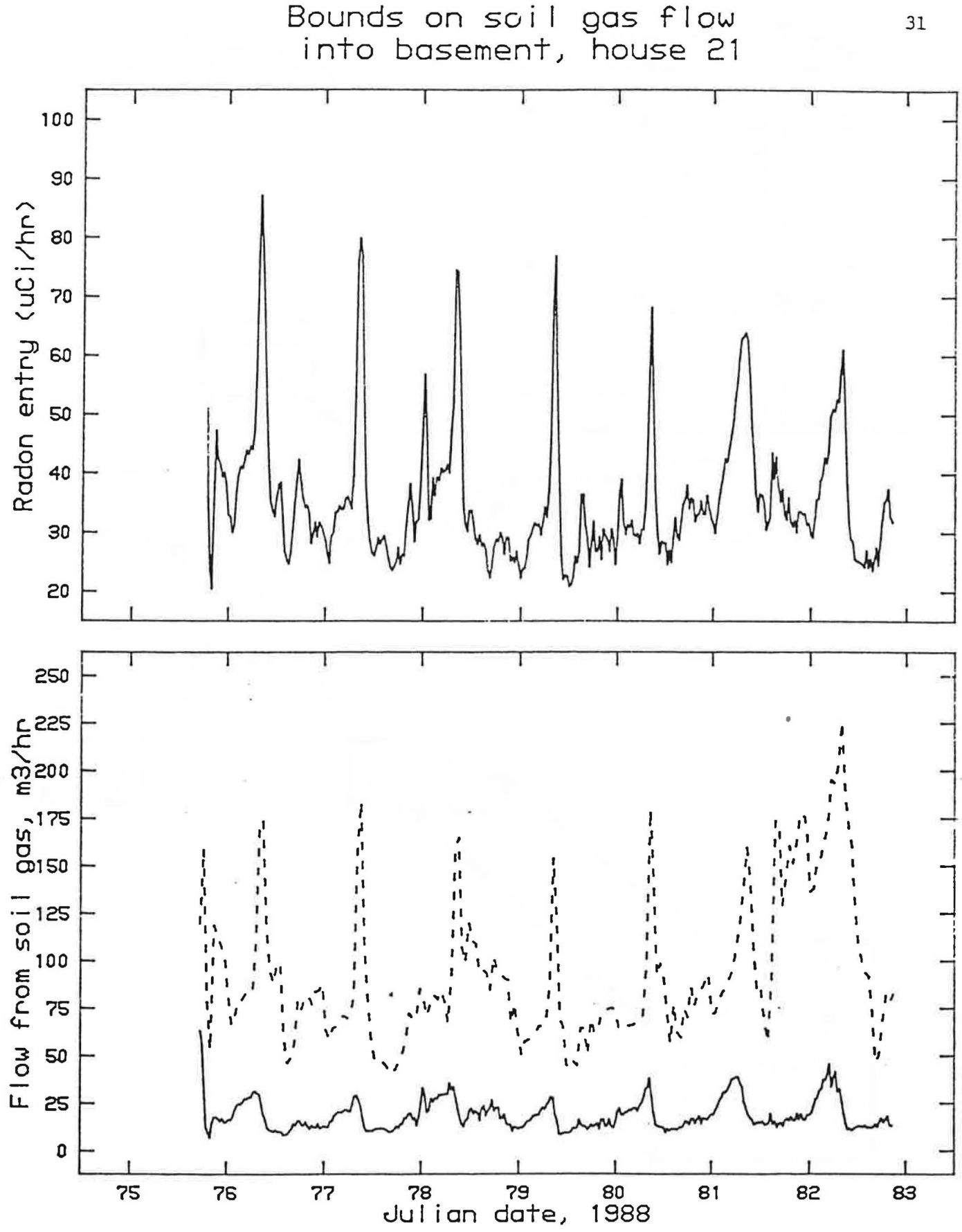
Bounds on soil gas flow into basement, house 21
Radon entry (uCi/hr)
100
90
80
70
60
50
40
30
20
Flow from soil gas, m3/hr
250
225
200
175
150
125
100
75
50
25
0
75
76
77
78
79
80
81
82
83
Julian date, 1988
(Rn entry/[Rn] subslab)
total measured flow from outside

Figure 5

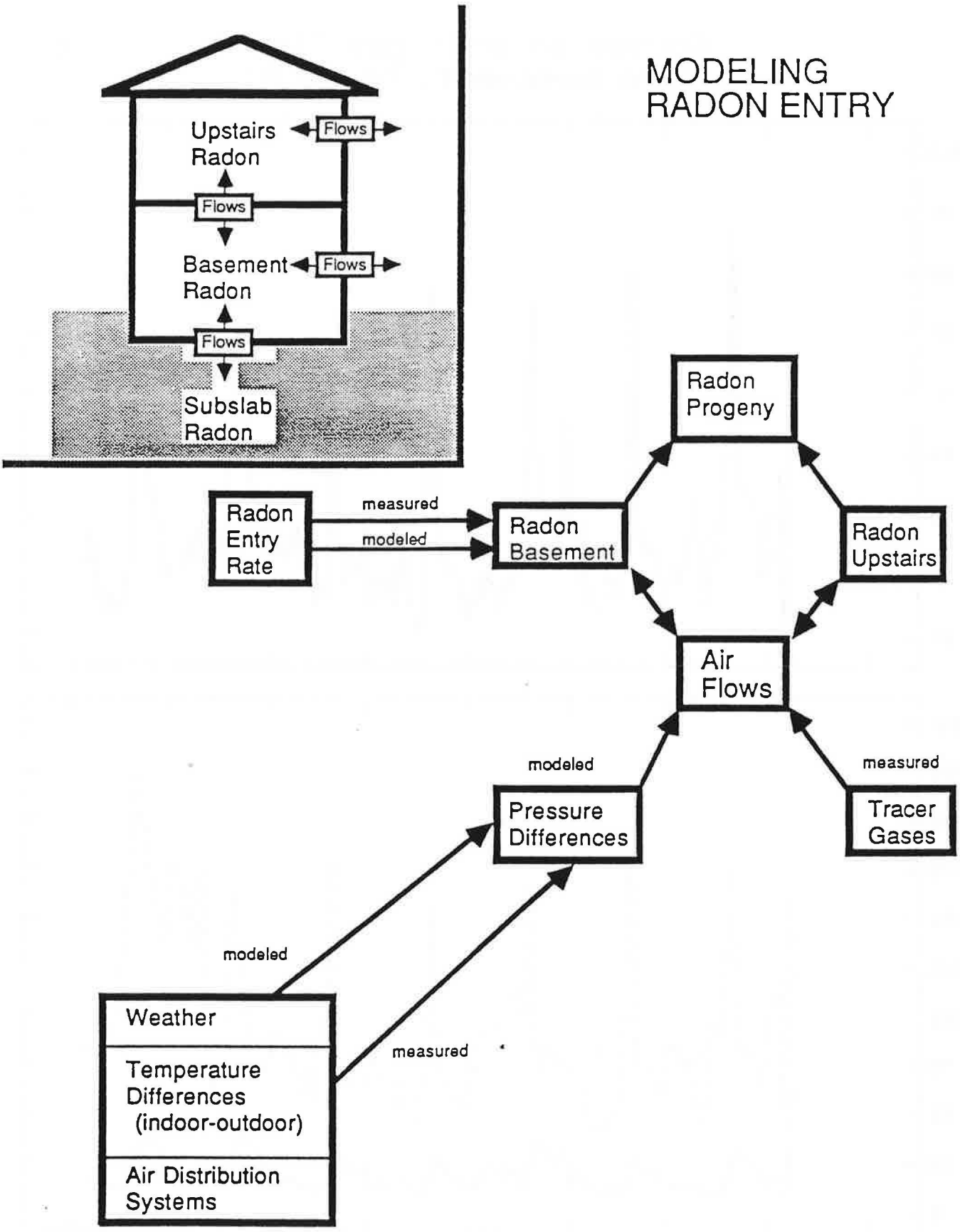
MODELING
RADON ENTRY
Upstairs
Radon
Flows
Flows
Basement
Radon
Flows
Flows
Subslab
Radon
Radon
Progeny
Radon
Entry
Rate
measured
modeled
Radon
Basement
Radon
Upstairs
Air
Flows
modeled
measured
Pressure
Differences
Tracer
Gases
modeled
measured
Weather
Temperature
Differences
(indoor-outdoor)
Air Distribution
Systems

Figure 6

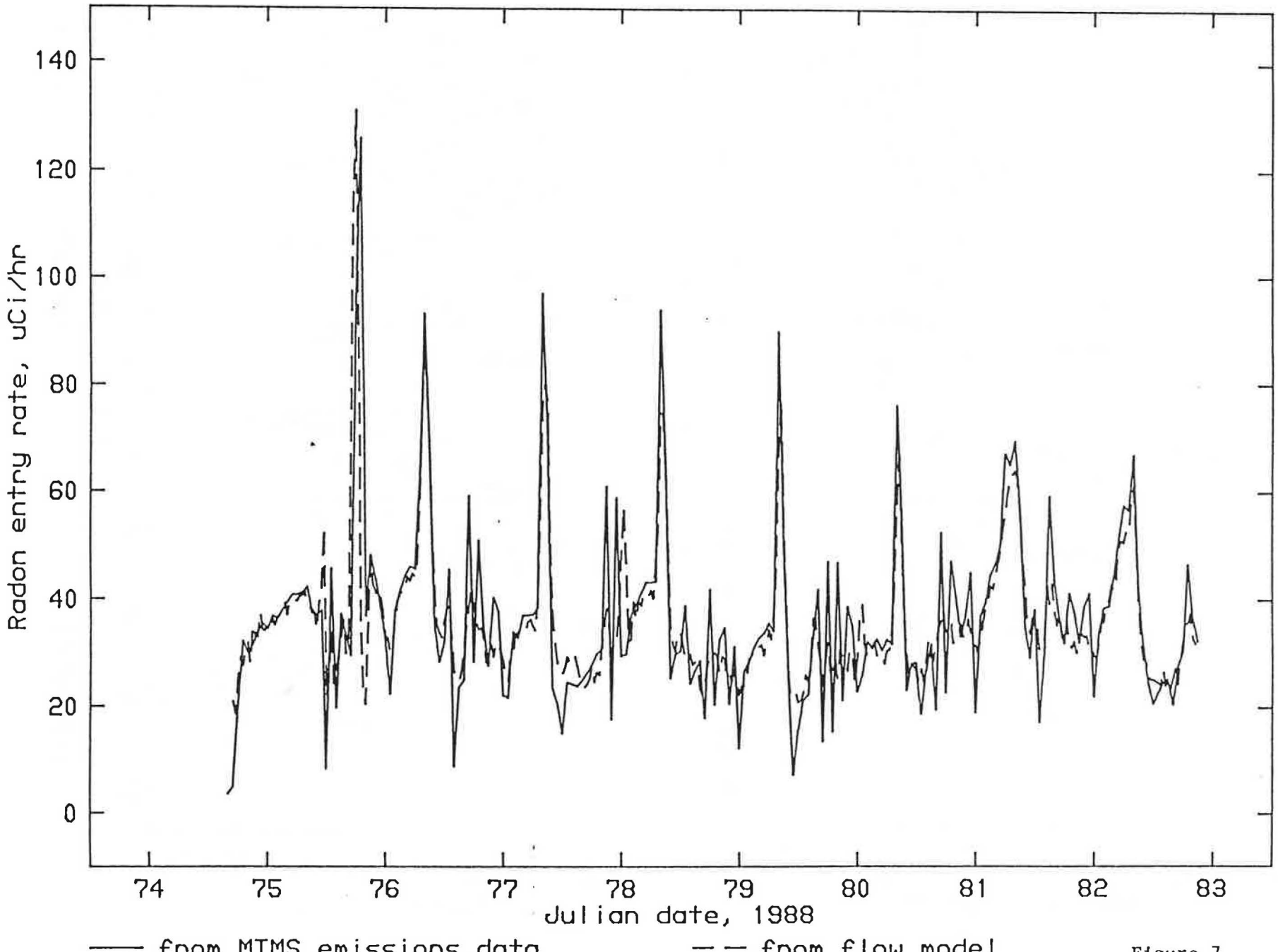
140
120
100
80
60
40
20
0
Radon entry rate, uCi/hr
74
75
76
77
78
79
80
81
82
83
Julian date, 1988
from MTMS emissions data
from flow model

Figure 7

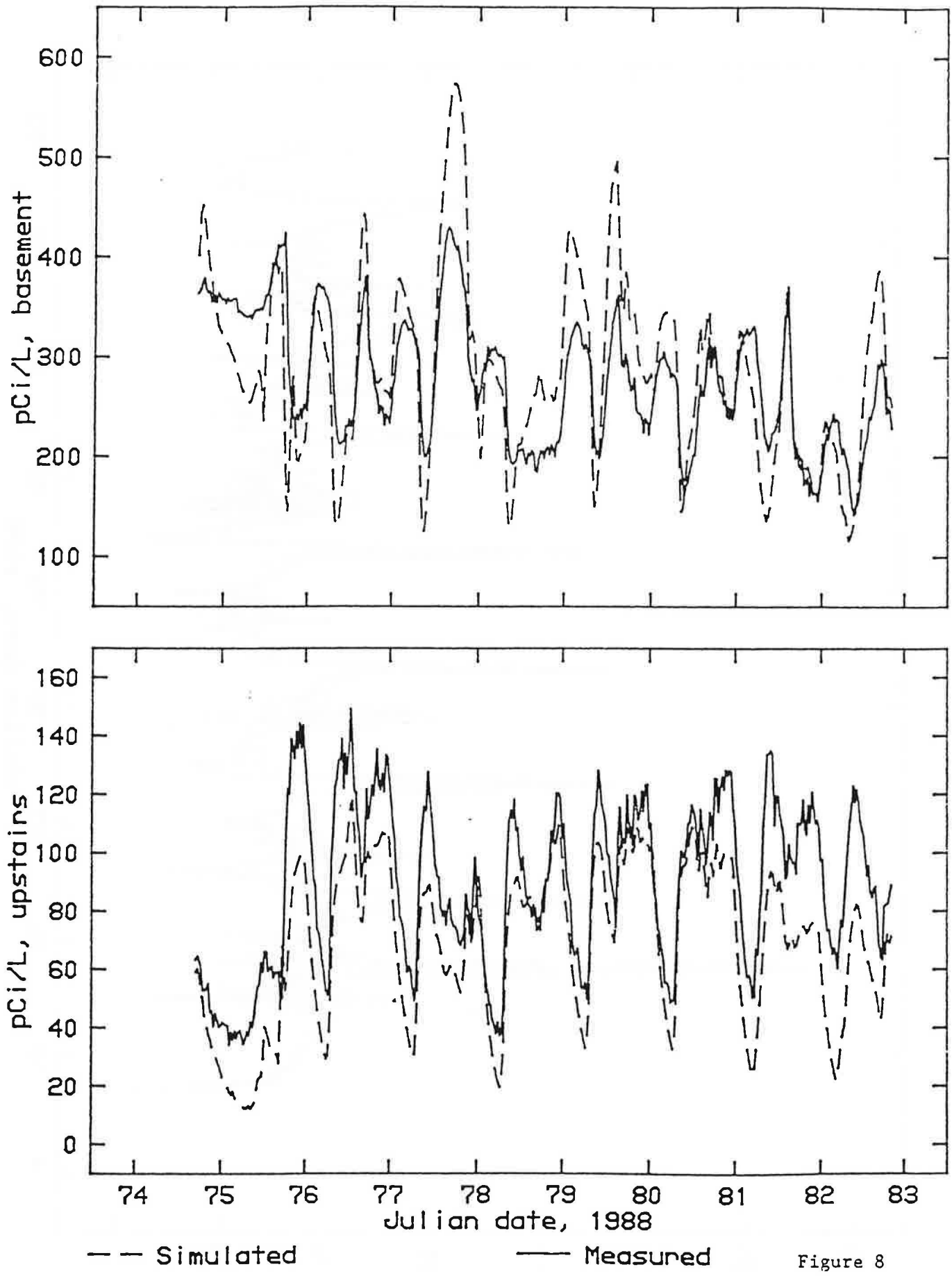
600
500
400
300
200
100
pCi/L, basement
160
140
120
100
80
60
40
20
0
pCi/L, upstairs
74
75
76
77
78
79
80
81
82
83
Julian date, 1988
Simulated
Measured

Figure 8

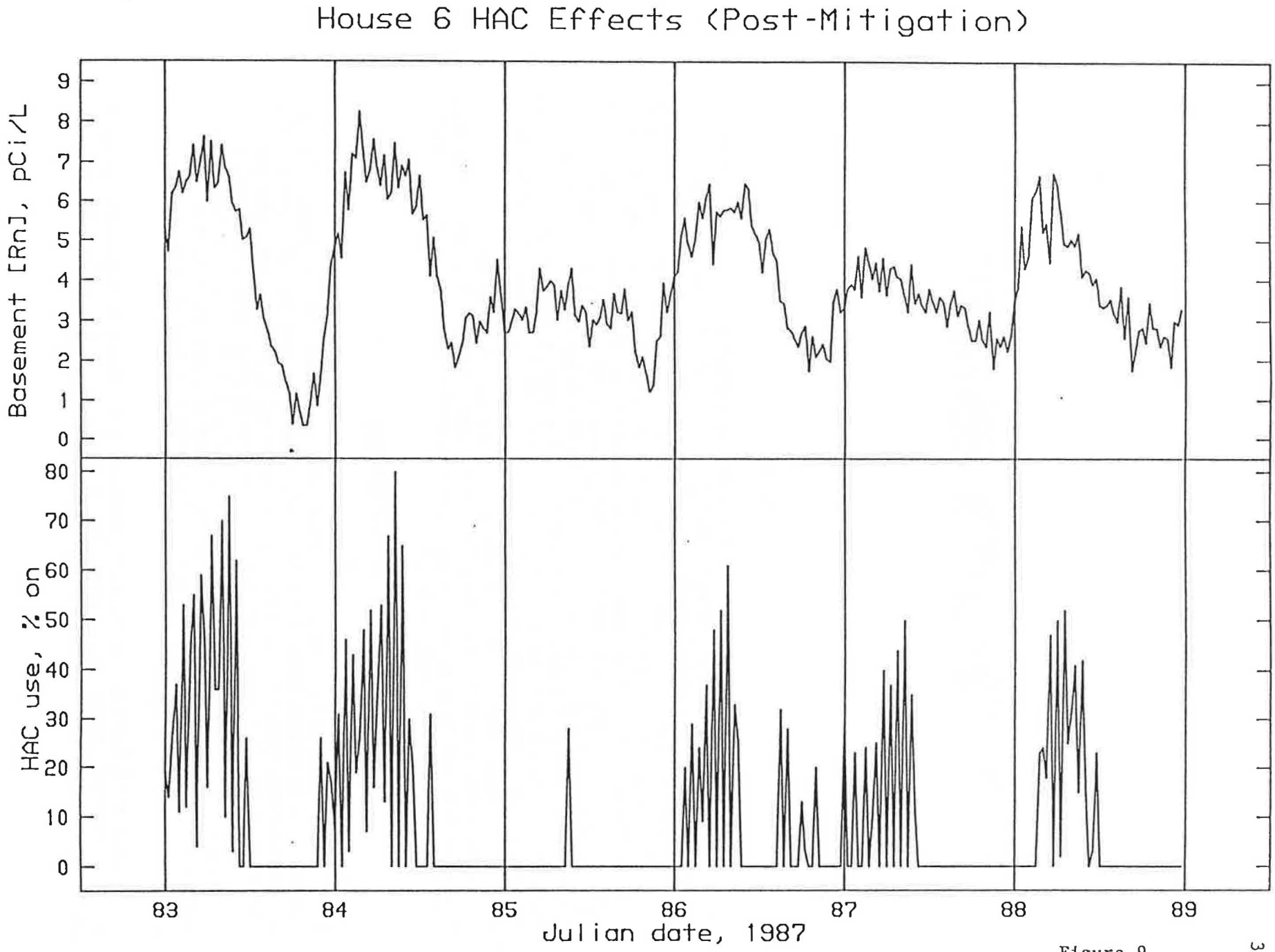
House 6 HAC Effects (Post-Mitigation)
Basement [Rn], pCi/L
0
1
2
3
4
5
6
7
8
9
HAC use, % on
0
10
20
30
40
50
60
70
80
83
84
85
86
87
88
89
Julian date, 1987

Figure 9

PART B - RAPID DIAGNOSTICS: SUBSLAB AND WALL DEPRESSURIZATION SYSTEMS FOR CONTROL OF INDOOR RADON

Abstract

Design and implementation of a rapid diagnostic protocol for subslab and wall depressurization systems designed to control indoor radon is currently being developed in New Jersey homes. The protocol leads to a distinction between hard and easy homes to mitigate using the subslab and wall depressurization approach, and facilitates efficient design of the mititigation system. This paper discusses parts of the research which have been used to develop the protocol, and presents the diagnostic protocol itself. Specifically discussed are data on the airflow characteristics associated with the soil gas beneath the slab and beyond the basement walls that define "good communication"; i.e., connectivity. The manner in which these characteristics are translated into a protocol that is practical for use by professionals in the private sector is also discussed.

This paper has been reviewed in accordance with the U.S. Environmental Protection Agency's peer and administrative review policies and approved for presentation and publication.[1]

I. INTRODUCTION

The mitigation technique we have found most useful in the New Jersey homes studied in the Piedmont and Princeton Projects (1) has been subslab and/or wall depressurization (SSD). Why should we perform diagnostics for SSD mitigation systems? Wouldn't it be more efficient to just mitigate rather than "waste" time testing? The answer is that the use of proper diagnostic procedures can reduce the cost of mitigation by providing the information needed by the mitigator to choose the fan size needed, the number and proper location of penetrations through the slab or walls, and

---

[1]This work has been funded cooperatively by the New Jersey Department of Environmental Protection, Identification No. 258761, and the United States Environmental Protection Agency, CR-814673-01-0.

the pipe size necessary to provide a system that should effectively reduce the radon levels to an acceptable level, the first time around. We know that a large percentage of homes that have been mitigated are still above the recommended 4 pCi/L indoor radon concentration. A recent study (2) found that 64% of the homes in New Jersey where post-mitigation radon measurements have been taken remain above the recommended limit. (The post-mitigation measurements are not annual averages and are collected on the lowest floor of the home.) Diagnostics improve the success rate, thus lowering the cost to the building owner and the occupant's exposure to radon. Of course, the diagnostics may show that SSD is not the first choice for a particular structure, and alternate techniques will be required to achieve successful mitigation, but time and money will also be saved by this conclusion.

What do we mean by rapid diagnostics? Field studies in radon research during the past year and a half have placed considerable emphasis on development of diagnostic procedures (3). As the techniques have developed, the quality and sophistication of the measurements have increased (4). Along with this, the time spent performing the diagnostic tests has also increased, and we constantly find ourselves asking which measurements are truly useful to the private radon reduction business sector.

Based on the economics of the radon mitigation business, most mitigators won't want to spend more than 2 person hours on diagnostics in buildings that are simple to mitigate. Certainly the type of house construction and substructure will greatly influence the time required for diagnostics. Radon mitigation in a development, townhouse, or condominium community will probably require a full set of diagnostic measurements only on the first few buildings to determine the proper mitigation system installation and therefore reduce the overall diagnostic time per unit. At the easy end of the diagnostics scale is the housing development that has some homes built, and some still in various stages of construction. In this case inspection of the substructure as it is being built may give enough information, such as the existence of a well-defined gravel bed, to design an effective mitigation system. At the other extreme, where the diagnostic time is anticipated to be stretched out, is the older home with little evidence that gravel has been used under the slab or the home where basement, crawlspace, and slab-on-grade construction has been mixed.

II. CONNECTIVITY

One of the key diagnostic tests used for designing a SSD mitigation system determines the degree of connectivity under the slab(s). Connectivity in this context means the ability for a pressure and flow field to connect from one point to another beneath a slab, from slab to wall, or from wall to wall. The connectivity test can be briefly described as applying suction (usually with a vacuum cleaner) to a hole drilled through the subslab. Additional test holes drilled and temporarily capped are placed radially at a series of distances from the suction hole. The pressure difference across each test hole and velocity through each test

hole are measured as a function of varying the suction applied to the suction hole.

Connectivity can be very complex. For example, one should not confuse the achievement of significant airflows being exhausted from beneath the slab (at reasonable pressures through the vacuum cleaner) as an indication of good connectivity. If there is an easy path to the house perimeter drain, sump, or floor drain, high airflows will result but connectivity under the slab may be marginal or even non-existent. A favorable characteristic is that these reasonable flows do not come from a few short circuit paths but rather represent soil gas flowing radially under the slab from the area surrounding the suction point. A short circuit is a lower resistance path inside a higher resistance medium that allows air from outside the subslab to flow to the suction hole.

Establishment of reasonable flow ensures that the subslab will be appropriately depressurized. Lowering the subslab pressure below that of the basement/crawlspace/living space prevents the radon-laden soil gas from moving into the building. The actual flows achieved with the subslab depressurization system in operation need be large enough only to establish the desired subslab depressurized field. The pressure difference across the slab must be large enough to overcome the stack effect, the effect of wind speed and direction, or the effect of heating and air conditioning (HAC) depressurization of the substructure, all of which allow the radon to enter through pressure driven flow. The average values of the pressure differences created by the aforementioned effects are typically between 1 and 5 Pa, although a very poorly balanced air distribution system can create even higher pressure differences (1).

III. TESTING PROTOCOL

Returning to the practical world of time and money, we must examine exactly where a diagnostic protocol fits into the mitigation effort. Clearly a visual inspection is necessary in every case (3). Practical considerations of where the mitigation system can be installed, where suction holes can be placed, and where the discharge points for the exhaust of the soil gas can be located, must all be factored into the diagnostics. The fact that soil gases must be exhausted in a way to prevent reentry into the living space cannot be overlooked. Preferred discharge points would be through the roof of the building or attached garage. These considerations are now addressed in the following protocol for subslab depressurization diagnostics.

PRINCETON PRE-MITIGATION RAPID DIAGNOSTICS PROTOCOL

Building Structure

- [ ] Visual inspection of the interior and exterior of the building.

During the building inspection decide on a convenient location (or

locations) to place the mitigation pipe(s) and the penetrations(s) into the slab. Criteria for this decision include:

- [ ] Look for a slab penetration point which is near a convenient basement (or crawlspace) exit point. Convenient exit points are, for example, through a band joist to an adjoining garage which allows venting through the roof.

- [ ] Look for a slab penetration point which allows access to the complete subslab area without blockage from footings, piping (especially determine where the water, sewer, and gas lines enter), or duct work under the slab.

- [ ] Look for a slab penetration point which places the mitigation piping in the most unobtrusive position in the substructure as possible. Determine if straight runs of mitigation piping are possible, if practical, to minimize the use of pressure-robbing elbows and other fittings, and to avoid condensate collection in the piping.

Building Dynamics

- [ ] Drill a 1.5 in. diameter hole through the slab approximately 5-6 in. away from the wall, assuming that your choice of exit point is near a wall, in the area of the subslab that appears to be the logical mitigation pipe exit point.*[2] If the mitigation fan is to be installed in the basement or crawlspace, the hole should be far enough away from the wall to allow installation, normally about 13 in. Vacuum the area in and around the hole to remove drilling debris. Inspect the area beneath the slab to try to determine the conditions that are present; e.g., gravel layer and condition, water presence, metal mesh, plastic barrier, mud, or other solid packed materials. Also check the area just beneath the slab to make sure that the drilling process didn't plug the slab/subslab interface. Plug the hole with similar diameter backer rod and rope caulk.

- [ ] Install the large 1.5 in. flow and pressure tube (FPT) into the hole and connect the vacuum cleaner suction hose. (The vacuum cleaner should be outdoors if possible or have the exhaust side vented outdoors since high concentrations of radon gas are present in the vacuum exhaust. A 2.5 in. hose should be used to minimize the hose pressure drop.) Attach the "low" side of the pressure instrument to the lower pressure tap of the test device. Connect the speed control to the vacuum cleaner and slowly bring the speed up until you achieve 500 Pa static pressure difference between the basement and the 1.5 in. FPT or until you reach the maximum speed setting. Note the static pressure difference reading (in inches of water)

---

[2] This distance is chosen to avoid the footing, but still take advantage of any falling away of the soil and gravel at the building perimeter (anticipated because of building activity near the footing during building construction). Table 4 gives metric equivalents.

on the data sheet (Table 1). The measurement in inches of water, with a resolution of 0.001 in., is preferred. Connect the velocity port of the pitot tube to the "high" side of the pressure instrument, and the static pressure port of the pitot tube to the "low" side of the instrument; then note the reading (in. H_2O) on the data sheet. Turn vacuum cleaner off.

Calculate the average velocity (V) of the flow (Q):

$V = 1096.7 \times \sqrt{(h/d)}$

Where:

V = velocity, ft/min.
h = velocity pressure, in. H_2O
d = density of air, lb/ft^3
1096.7 = unit conversion factor

Calculate the flow (Q):

$Q = AxV$

Where:

Q = ft^3/min.
A = cross sectional area of the tube, ft^2
V = average velocity, ft/min

Or use the flow chart (a portion of which is shown in Table 2) to determine the flow.

If the flows seem reasonable (e.g., more than 20 cfm with pressures of 500 Pa, but less than 50 cfm), then drill a 0.5 in. diameter hole through the slab at the most distant point from the 1.5 in. diameter hole, again penetrating the slab about 5-6 in. from the wall. A high flow rate from the suction hole with a low pressure differential could be an indicator of the flow bypassing the subslab area and short circuiting to air from outside this area. A low flow from the suction hole, combined with a high differential pressure, indicates poor connectivity.

- [ ] After vacuuming the drilling debris from in and around the 0.5 in. hole install the 0.75 in. FPT over the hole. With the plug in place and the pressure port connected to the pressure measuring instrument, repeat the previous settings of the vacuum and note the 1.5 in. FPT static and pitot pressures and the 0.75 in. FPT static pressure difference.

- [ ] Remove the plug and note the 1.5 in. FPT parameters along with the velocity measurement in the 0.75 in. FPT. If the velocity is more than 10 ft/min and the 0.75 in. FPT static pressure difference is 0.004 in. H_2O or greater, then good connectivity is indicated and a subslab depressurization system can be installed without further pre-installation diagnostics.

Note: If the pressure or velocity measured at the reference hole is below the above recommendations, then further diagnostics are required. These would include pressure field extension measurements (see section IV), subslab and wall radon grab samples, and wall pressure difference measurements.

When testing a slab with a perimeter drain, sometimes short circuiting to the drain from the suction hole will occur. Seeing if smoke will be drawn into the subslab area through this drain at some distance (e.g., 15 ft) from the suction hole indicates good connectivity, and a subslab depressurization system can be installed.

• [ ] Appliance cycling - Substructure vs outside pressure differential measurements as appliances are cycled on and off.

[ ] furnace or central AC -----
- [ ] fan only
- [ ] combustion only
- [ ] both above

[ ] exhaust fans (range, especially the Jenn Aire type range vent)

Record the pressures on the data sheet. If $\Delta P_{s-b}{}^{furn} > \Delta P_{s-b}{}^{vac}$, the mitigation system could be ineffective during the appliance operation. This means "if the static pressure differences between the subslab and the basement, when the furnace or other appliance is operating, is greater than those measured with the vacuum operating during the previous protocol."

EQUIPMENT NEEDS FOR CONNECTIVITY TESTING

An important ingredient of the diagnostic protocol is making the connectivity measurements. Equipment needed includes an industrial vacuum cleaner capable of 95 cfm at a 2.0 in. orifice and 75 in. H_2O static vacuum pressure, a pressure measuring device with a resolution of 0.001 in. water and a range to 20 in. H_2O, an anemometer to measure velocities from 10 to 3000 ft/min, a speed control to vary the vacuum cleaner flow and suction, and a rotary hammer drill to drill holes of up to 1.5 in. diameter through 4 to 6 in. concrete slabs.

Other equipment used are the 1.5 and 0.75 in. Flow and Pressure Tubes (FPTs) described below and shown in Figure 1. These devices allow us to measure the pressures and flows developed by the controlled vacuum cleaner and to measure the pressure difference between the subslab and the basement and flows into the test holes. The 1.5 in. FPT has a port on the upper end in which to install a pitot tube to measure velocities in the tube that can be used to calculate the flow rate, and a port at the lower end to measure the pressure developed. We do not use an anemometer to measure velocities in the 1.5 in. FPT because, during operation of the vacuum, foreign material may be drawn into the tube which will destroy the probe. Other design features of the 1.5 in. FPT are that it extends only 3 in. into the slab so that it does not penetrate through the slab and block off the slab/subslab interface, and that the heavy weight on the lower section ensures that the large O-ring seals properly to the floor. The 0.75 in. FPT has a port on the upper end where an anemometer is installed to measure the flow into the test hole. The anemometer is used here because the flow is from the inside of the substructure into the test hole and therefore shouldn't pose any hazard to the probe. There is also a port on the lower section of the tube to measure the pressures. A rubber stopper is used to

plug the inlet (top) end of the tube when subslab static pressures are being measured. The heavy weight and O-ring are also used in this design.

EXAMPLE OF CHOOSING THE SSD MITIGATION SUCTION HOLE LOCATION

To demonstrate the change in the pressure difference between the basement and the subslab at various distances from a suction hole, during different house conditions, Figure 2 shows the pressure difference across three floor test holes during pre-mitigation diagnostics and after mitigation. The basement is the reference pressure. The ordinate is the difference between the subslab pressure and the basement pressure; a negative pressure means the subslab is depressurized relative to the basement. Five different tests are presented, as shown in the key on the figure. During the pre-mitigation diagnostics we tested the airflow communications by suction on both the sump and floor hole F6, shown in the floorplan (see Figure 3). Both of these are convenient locations for placement of the subslab suction, as determined during the building inspection, discussed below.

The first two bars above each floor hole in Figure 2 are the pressure differences in the three test holes with: 1) the variable speed vacuum on F6, labeled F6=-290, and 2) the variable speed vacuum on the sump, labeled sump=-290. Both suction airflows were achieved through 1.5 in. holes, drilled through the slab at F6 and drilled into a temporary sump cover at the sump. A 1.5 in. tube was connected to the hole, and the vacuum cleaner suction tube was connected to the tube. The number -290 refers to the pressure difference at the suction hole between the inside of the 1.5 in. tube and the basement, expressed in pascals. All test holes other than the suction holes are 0.5 in. diameter. Suction at F6 gave a measurable pressure difference at each floor hole, but suction at the sump gave no measurable pressure difference at test hole F5. Thus the installed mitigation system used F6 as the suction hole.

PRESSURE DIFFERENCES UNDER VARIOUS HOUSE OPERATING CONDITIONS

The other three columns above each test hole in Figure 2 show the pressure differences measured under different conditions after the mitigation system was installed. The positive pressure difference measured with the mitigation system off and the air conditioner (AC) running means that the basement is depressurized relative to the subslab soil gas. When the mitigation system is running and the air conditioner is on (versus off), the effect of the basement depressurization caused by the air conditioner air handler is evident. In both cases, however, the subslab remains depressurized relative to the basement, so that these added negative stresses on the mitigation system are not significant in this house. The pressure difference between the inside of the 4 in. diameter mitigation pipe and the basement is shown in the key (as F6=-276 Pa). Note that the pre-mitigation pressures at the suction point are taken between the basement and inside a 1.5 in. pipe and, after mitigation is installed, the measurements are between the inside of a 4 in. pipe and the basement. Also note from Figure 3 that F3 is the farthest hole from F6, so that the

decrease in intensity of the pressure differences between holes is consistent with the distance of each hole from the suction point.

PRECAUTIONS

Weather effects and HAC interactions (5) may interfere with the diagnostic results. An example of rain influencing the pressure difference readings is seen in Figure 4. Pressure differences between the basement and subslab increased 4 to 20 times under the wet conditions as compared to dry conditions. Changes of this magnitude could present problems in diagnostic data interpretation and lead to erroneous mitigation system design.

IV. PRESSURE FIELD EXTENSION

Using a series of test holes radiating from the suction hole and measuring pressure differentials between the basement and subslab, a gradual drop in pressure as the distance from the suction hole increases is the expected result if the subslab contains a homogeneous flow field. If the pressure differential suddenly falls to zero with distance, blockage of the subslab flow passages is indicated. If there are noticeable deviations in the way the pressure differential falls with distance, depending upon the radial orientation of the test holes, nonuniformity of the gravel bed is evident. Slower decreases in pressure, such as in a linear falloff, may indicate an easier flow path or short circuit. Since flow is not confined to the specific radial direction being measured, these simple profiles, as illustrated in Figure 5, will be modified by flows from other circumferential directions.

How are the pressure and flow data that are critical to conductivity testing interpreted? As previously discussed, we measure pressure differences between the basement and subslab at each test hole (on various rays extending from the suction hole as shown in Figure 6). We are also able to measure the flow through the test hole by removing the plug from the 0.75 in. flow and pressure tube (FPT) as outlined in the protocol. The way in which these data, as listed in Table 3, describe the airflow field under the basement slab is described in the following paragraphs.

PRESSURE DIFFERENCES

There can be significant variations in pressure profiles measured in different radial directions from a test suction hole. The following data help visualize the variation. Assume that the gravel layer beneath the slab is bounded on the top by the concrete slab and on the bottom by the earth below. We know that the airflow under the slab through a cross-sectional area surrounding the suction hole is equal at all radii. The cross-sectional area at each radial distance from the test suction hole is $2\pi r$ times the height of the aggregate times an effective area fraction (which is the fractional area not blocked by stones, sand, water, etc.). The subslab flow characteristics can be evaluated with the help of the following relationship between the flow (Q) and the pressure difference (ΔP):

$$Q \propto A x \Delta P^n$$ where: Q = flow,

A = effective area,
ΔP = pressure difference across the slab,

and n is assumed to be 0.65, similar to the pressure and flow relationship found during pressurization measurements of building shells (6) and close to the values of the ORNL subslab test (7). Assuming a homogeneous subslab with uniform flow characteristics in all directions, the anticipated pressures at test holes F6, F7, and F8 are approximately 7 times the pressures at F3, F4, and F5, repectively, based on the radial distances from the suction hole (reported in Table 3). Uniform flow characteristics under the slab would result in similar pressure differences measured at similar radial distances from the central test suction hole. Applying suction at the 1.5 in. hole (marked V in Figure 6) and measuring the pressure and flow data at each test hole (reported in Table 3), the additive pressures[3] at the near test hole divided by the additive pressures at the far test hole can be compared. These ratios are 20 (pressures at hole F7/pressures at hole F5), 8 (pressures at hole F8/pressures at hole F3), and 3 (pressures at hole F6/pressures at hole F4). Without knowing any flow data, these numbers can be interpreted as implying 1) that a higher than expected flow exists from F6 to F4 (because of the lower than expected pressure ratio reported in Table 3), 2) that the flow from F8 to F3 is close to the expected flow, because the pressure ratio is close to the expected value, and 3) that the flow path between F7 and F5 is greater than the expected ratio, indicating possible blockage.

FLOW

At test hole F4 (with the plug removed from the 0.75 in. FPT) the measured flow is more than an order of magnitude greater than at test hole F3 or F5. The flows are 1.07, 0.61, and 0.49 cfm at test hole F4, for 2000, 1000, and 500 Pa suction, respectively; versus 0.07, 0.03, and 0.01 cfm at test hole F3 and 0.06, 0.02, and 0.01 cfm at test hole F5 (see Table 3). Thus the flow measurements confirm the pressure ratio data which indicates blockage in the path from F7 to F5, and a good flow path between F6 and F4. In addition, the flow data also point out blockage in the F8 to F3 path that would not have been clear based on the comparison of the pressure measurements alone. (The flow data indicate similar flows from F7 to F5 and from F8 to F3.) When the flows are measured at test holes F6, F7, and F8, they show that, for the last 3 ft of flow path to the suction hole, the path to F8 is preferred rather than the path to F6. The flows are 1.8, 1.3, and 0.98 cfm for test hole F8, 1.25, 0.83, and 0.64 cfm for test hole F6, and 0.36, 0.22, and 0.14 cfm for test hole F7 at the three suction pressures of 2000, 1000, and 500 Pa. Again these diagnostics have pointed out the degree of nonuniformity in flow through the gravel bed from three

---

[3]The pressure differences at each test hole in the series of connectivity tests reported in Table 3 are added to minimize the effect of measurement errors. The test equipment has a minimum resolution of 1 Pa on the range used for these tests.

different directions to the suction hole, with a variable preference in flow path depending on the distance from the suction hole.

Summary. Flow measurements can be used to substantiate the pressure ratio information and indicate nonuniformities of the gravel bed flow path. Because the final subslab pressure field is the goal of the subslab/wall depressurization mitigation approach, pressure measurements are particularly required at the farthest test holes from the suction point to ensure that all of the subslab has been depressurized by the mitigation fan suction.

V. CONCLUSIONS

Diagnostic protocols for subslab and wall depressurization mitigation systems can lead to more effective radon mitigation system design and installation at a lower final cost to the building owner. A series of pre-mitigation diagnostic procedures has been suggested as a way in which to evaluate a building for a SSD mitigation system. This paper has presented a protocol for diagnostics in a situation where a gravel bed is present beneath the slab (basement, crawl space, or slab-on-grade). This protocol makes use of several pressure and flow measurement techniques to evaluate the subslab airflow characteristics. The influence of house appliances, especially heating and air conditioning equipment, is also evaluated to determine their possible influences on SSD mitigation system operation. Examples of some of the influences of weather (rain) and nonuniformities of the gravel bed on the diagnostics have also been discussed. If the subslab conditions are fairly uniform, measurements of pressure differences between the subslab and the basement may be the only pre-installation diagnostics required to properly determine the radon mitigation system design. As the conditions beneath the slab vary from homogeneity, then flow measurements such as those described in this paper become important in determining the proper system design. The combination of pressure and flow measurements will provide the data to help us better understand the subslab conditions that are found by the mitigator and researcher. Standardization of measurement parameters and units of measure is also important. Measuring pressure differences in inches of water and velocities in feet per minute would give better resolution on most of the instruments available presently and reduce many of the questionable measurements reported.

REFERENCES

1. Matthews, T.G. et al. from ORNL and Hubbard, L.M. et al. from Princeton University, " Investigation of Radon Entry and Effectiveness of Mitigation Measures in Seven Houses in New Jersey," mid-project report, ORNL/TM-10671, June 1988.

2. Wang, J., Cahill, M., "Radon Reduction Efforts in New Jersey," paper presented at Annual Meeting of the National Health Physics Society, Boston, MA, July 4-8, 1988.

3. Dudney, C.S., Hubbard, L.M., Matthews, T.G., Socolow, R.H., Hawthorne, A.R., Gadsby, K.J., Harrje, D.T., Bohac, D.L., Wilson, D.L., "Investigation of Radon Entry and Effectiveness of Mitigation Measures in Seven Houses in New Jersey," Final report, ORNL-6487, September 1988.

4. Turk, B.H., Harrison, J., Prill, R.J., Sextro, R.J., "Preliminary Diagnostic Procedures for Radon Control," EPA-600/8-88-084 (NTIS PB88-225115), June 1988.

5. Hubbard, L.M., Bolker, B., Socolow, R.H., Dickerhoff, D., Mosley, R.B., "Radon Dynamics in a House Heated Alternately By Forced Air and By Electric Resistance," U.S. EPA 1988 Symposium on Radon and Radon Reduction Technology, Denver, CO, October 1988.

6. Jacobson, D., Harrje, D.T., Dutt, G.S., " Measurement of Air Leakage Properties of Common Residential Insulating Materials," ASTM Conference on Thermal Insulation, Materials and Systems, Dallas, TX, December 1984.

7. Matthews, T.G., personal communication, September 1988.

Table 1. Data Sheet for Subslab Connectivity Diagnostics

House No._____ Investigator_____ Date_____

Location of suction hole_____

All Pressure Readings, in. H_2O

Vacuum Settings, test holes plugged				Vacuum Settings, test hole open			
Delta P	Pitot P	Vel., fpm	Flow, cfm	Delta P	Pitot P	Vel., fpm	Flow, cfm

TEST HOLE DATA
Vacuum Delta P _____ _____ _____

Hole No.	Distance	DP, plugged	DP, open	Vel, fpm	Flow, cfm

APPLIANCE CYCLING Substructure vs outside pressure difference

Furnace or central AC------ fan only _____ in. H_2O

combustion only _____ in. H_2O

both of the above _____ in. H_2O

Exhaust fans Location _____ _____ in. H_2O

Location _____ _____ in. H_2O

Table 2. Diagnostics Flow Chart

VELOCITY AND FLOW CHART FOR SUBSLAB DIAGNOSTICS[4]

		PITOT TUBE				ANEMOMETER		
PRESS. In.H20	VEL. Ft/m	FLOW 1.5FPT	FLOW 0.75FPT	FLOW 4in.Pipe	VEL. Ft/m	FLOW 1.5FPT	FLOW 0.75FPT	FLOW 4in.Pipe
0.01	400	4.47	1.02	35	59.0	0.66	0.15	5
0.02	566	6.32	1.44	49	88.6	0.98	0.22	8
0.03	694	7.74	1.76	61	118.1	1.31	0.29	10
0.04	801	8.93	2.03	70	147.6	1.64	0.37	13
0.05	895	9.99	2.27	78	177.2	1.97	0.44	15
0.06	981	10.94	2.49	86	206.7	2.29	0.52	18
0.07	1060	11.82	2.69	92	236.2	2.62	0.59	21
0.08	1133	12.63	2.87	99	265.8	2.95	0.66	23
0.09	1201	13.40	3.05	105	295.3	3.28	0.74	26
0.10	1266	14.12	3.21	111	324.8	3.60	0.81	28
0.11	1328	14.81	3.37	116	354.3	3.93	0.88	31
0.12	1387	15.47	3.52	121	383.9	4.26	0.96	33
0.13	1444	16.10	3.66	126	413.4	4.59	1.03	36
0.14	1498	16.71	3.80	131	442.9	4.91	1.10	38
0.15	1551	17.30	3.93	135	472.5	5.24	1.18	41
0.16	1602	17.87	4.06	140	502.0	5.57	1.25	44
0.17	1651	18.42	4.19	144	531.5	5.90	1.33	46
0.18	1699	18.95	4.31	148	561.0	6.22	1.40	49
0.19	1746	19.47	4.43	152	590.6	6.55	1.47	51
0.20	1791	19.97	4.54	156	620.1	6.88	1.55	54
0.22	1878	20.95	4.77	164	649.6	7.21	1.62	56
0.24	1962	21.88	4.98	171	679.2	7.53	1.69	59
0.26	2042	22.77	5.18	178	708.7	7.86	1.77	62
0.28	2119	23.63	5.38	185	738.2	8.19	1.84	64
0.30	2193	24.46	5.56	191	767.7	8.52	1.91	67
0.32	2265	25.27	5.75	198	797.3	8.84	1.99	69
0.34	2335	26.04	5.92	204	826.8	9.17	2.06	72
0.36	2403	26.80	6.10	210	856.3	9.50	2.14	74
0.38	2469	27.53	6.26	215	885.9	9.83	2.21	77
0.40	2533	28.25	6.43	221	915.4	10.15	2.28	79
0.42	2595	28.95	6.58	226	944.9	10.48	2.36	82
0.44	2656	29.63	6.74	232	974.4	10.81	2.43	85
0.46	2716	30.29	6.89	237	1004.0	11.14	2.50	87
0.48	2774	30.94	7.04	242	1033.5	11.46	2.58	90
0.50	2832	31.58	7.18	247	1063.0	11.79	2.65	92
0.52	2888	32.21	7.33	252	1092.6	12.12	2.72	95
0.54	2943	32.82	7.47	257	1122.1	12.45	2.80	97
0.56	2997	33.42	7.60	262	1151.6	12.77	2.87	100
0.58	3050	34.02	7.74	266	1181.2	13.10	2.95	103
0.60	3102	34.60	7.87	271	1210.7	13.43	3.02	105
0.62	3153	35.17	8.00	275	1240.2	13.76	3.09	108
0.64	3204	35.73	8.13	280	1269.7	14.08	3.17	110
0.66	3253	36.29	8.25	284	1299.3	14.41	3.24	113

[4] Approximate flow (ft^3/min.) for a one point measurement at the centerline of the tube or pipe.

Table 3. Typical Field Pressure/Flow Data

HOUSE 21 PRESSURE MAPPING

DATE	HOLE ID	DP*	VEL.†	FLOW‡	DIST.§	PITOT#	1.5FPT**
6/7/88	V	1002				0.71	37.63
	F2	0	0.0	0.00	16.83		
	F3	1	13.8	0.034	12.00		
	F4	6	246.1	0.613	11.25		
	F5	0	9.8	0.025	11.92		
	F6	23	334.7	0.834	3.25		
	F7	16	88.6	0.221	3.25		
	F8	16	531.5	1.32	3.25		
6/7/88	V	1780				1.70	58.23
	F2	0	0.0	0.00	16.83		
	F3	4	23.6	0.059	12.00		
	F4	11	338.6	0.844	11.25		
	F5	1	21.6	0.054	11.92		
	F6	37	433.1	1.08	3.25		
	F7	26	118.1	0.294	3.25		
	F8	27	669.3	1.67	3.25		
6/7/88	V	500				0.29	24.05
	F2	0	0.0	0.00	16.83		
	F3	1	5.9	0.015	12.00		
	F4	4	196.9	0.491	11.25		
	F5	0	5.9	0.015	11.92		
	F6	14	255.9	0.638	3.25		
	F7	10	57.1	0.142	3.25		
	F8	10	393.7	0.981	3.25		
8/18/88	V	2000				1.57	55.96
	F2	0	0.0	0.00	16.83		
	F3	4	27.5	0.069	12.00		
	F4	14	429.1	1.07	11.25		
	F5	2	25.6	0.064	11.92		
	F6	44	502.0	1.25	3.25		
	F7	30	145.7	0.363	3.25		
	F8	30	728.4	1.82	3.25		

*Static pressure (Pa) measured at the lower port of the 1.5 in. FPT on hole V or the pressure difference between the subslab and the basement measured at the pressure port of the 0.75 in. FPT.
†Velocity (ft/min) through the 0.75 in. FPT
‡Flow (ft^3/min) through the 0.75 in. FPT.
§Distance (ft) from suction hole V.
#Pitot tube pressure (in. H_2O) 1.5 in. FPT.
**Flow (ft^3/min) through 1.5 in. FPT at suction hole V.

Table 4. Metric Equivalence Data

1 pCi/L = 37 Bq/m^3
1 in. = 0.025 m
1 in. H_2O = 2.49 kPa
1 cfm = 0.00047 m^3/s
1 ft/min = 0.005 m/s
1 ft = 0.305 m

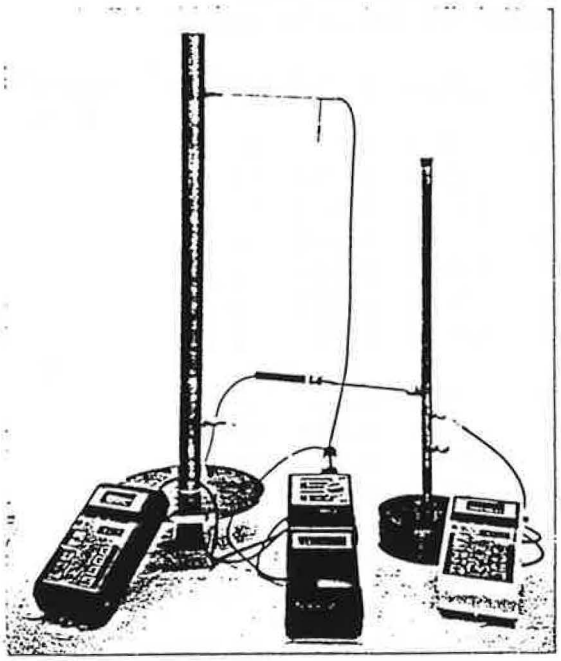

Figure 1. Two Flow Pressure Tubes (FPTs), 1.5 in. and 0.75 in. diameter (left to right), shown with electronic micromanometers, pitot tube, and electronic hot wire anemometer.

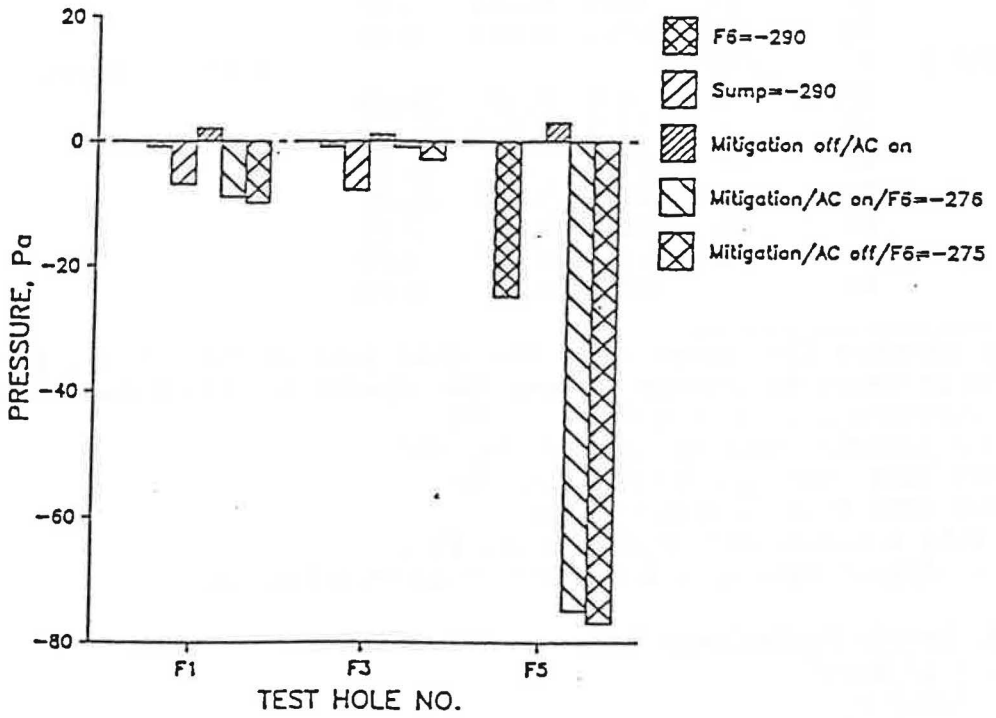

Figure 2. Pressure differences between the subslab and basement at three test holes in house No. 2 during pre-mitigation diagnostics and after mitigation under different HAC operating conditions.

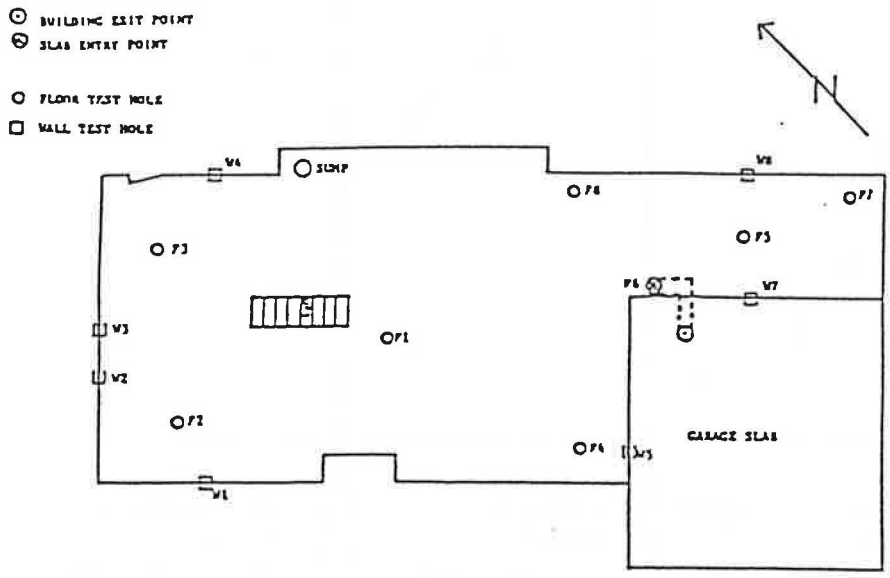

Figure 3. House No.2 basement floor plan showing the location of test holes, sump, and mitigation system slab penetration.

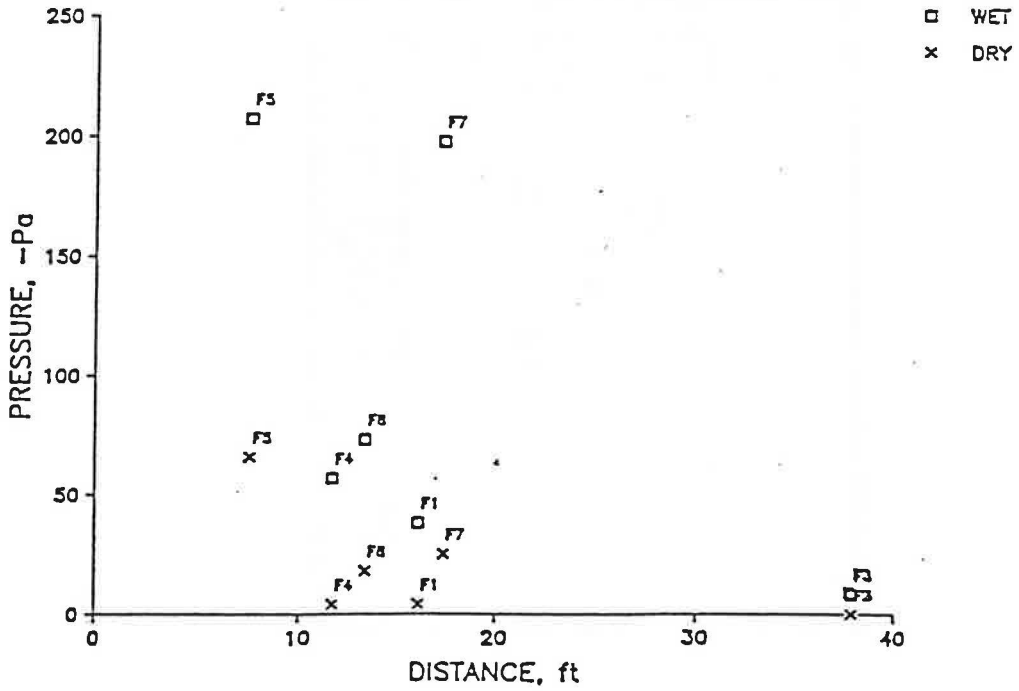

Figure 4. Post-mitigation pressure differentials between subslab and basement measured under wet (after rain) and dry conditions, house No. 2, same fan speed setting.

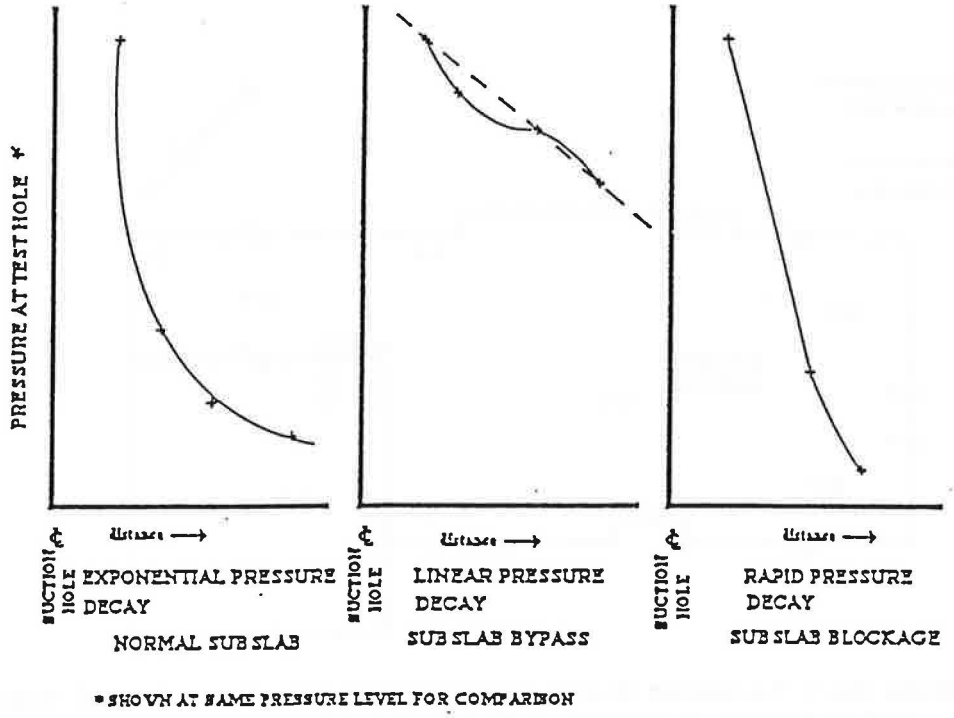

Figure 5. Pressure profiles in a test hole ray series extending from the suction hole.

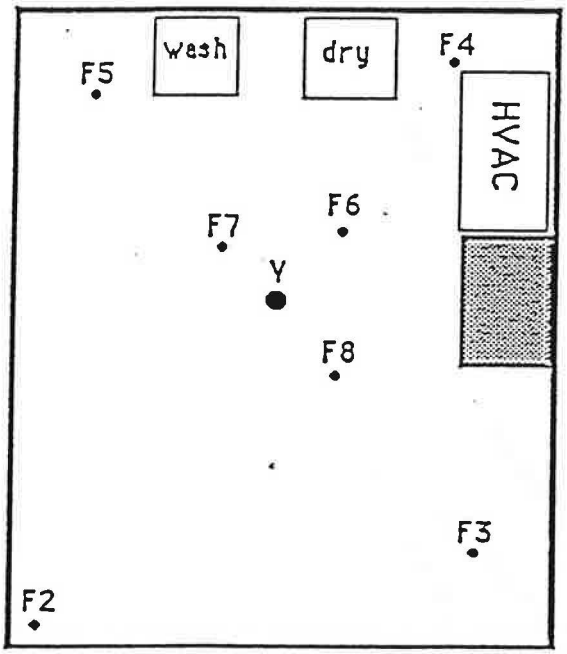

Figure 6. Basement floor plan indicating the location of the four rays of test holes extending from the suction hole (V).

APPENDIX A. ADDITIONAL DIAGNOSTIC MEASUREMENTS AND MITIGATION

MEASUREMENTS

There are three basic types of measurements taken during SSD pre-mitigation diagnostics. In the order of the increasing cost of equipment and level of expertise they are: pressure difference measurements, flow measurements, and radon grab sample measurements. Each of these testing procedures is done through the slab (basement floor or on-grade) or into the wall or block cavities. When the diagnostics indicate conditions other than a homogeneous subslab gravel layer are present, these more detailed and complete testing procedures become necessary.

Looking at the case of house 21, figure 7 shows the pressure differences between the basement and subslab at various test hole locations with suction pressures of 2000, 1000, and 500 Pa applied to hole V. These measurements lead to a different conclusion than you would get by adding the flow information as shown in figure 8 for the same set of test holes. The flow information helps to evaluate the permeability of the area beneath the slab and therefore provides an approximation of the capability of the mitigation system to move the radon gas from this critical space.

The addition of radon grab sample data, taken during ambient conditions with the furnace fan off, from these same test holes (Figure 9), indicates that most of the high radon readings are in the subslab zone with measurable flow characteristics. Hole number 2 is an exception and doesn't seem to have any connectivity to any other test holes but has a high radon reading. Testing of hole number 2 indicated almost no flow even at pressure differences up to 30 inches of water applied.

Additional connectivity testing was done by drilling a 1.5 inch hole through the slab in the southwest corner of the basement (F13), applying suction and taking measurements through some of the test holes. Hole F5 was also enlarged to 1.5 inches and similar measurements performed. The connectivity results from using F5 and F13 as the suction holes indicated less effective pressure and flow fields than those developed by applying the suction to hole V.

Information such as that just described presents the mitigator with the question of whether the high radon readings were an indication of the radon source, or whether in fact the readings were a result of a reservoir effect where radon gas from other location(s) were accumulating. In this case, the assumption was made that because of the relatively high readings of 2000 pCi/L, and the low permeability of this test hole zone, that the radon was the result of a small source that was not in good communication with dilution air.

Other testing included drilling a 1.5 inch hole into the wall at location W3 and measuring connectivity along the block wall. No pressure difference was measured at W1 even though smoke would be drawn into the hole. Communications around the wall corner to the north wall of the basement or to the south wall were nonexistent. The fireplace chimney walls

in the basement, figure 7, showed an interesting characteristic of oscillating pressures which indicated connections to the outside environment either through the attic or roof areas. All of the wall pressures were checked in two modes, furnace fan on and furnace fan off. The furnace fan had an effect on the pressures in the west basement wall adjacent to the living room slab. The pressure measured at W1 was 17 Pa higher during fan operation indicating that one or more of the supply ducts running to the living space slab through this wall was leaky. A look at the data (figure 10) points out a decrease in the wall concentration when the furnace fan is operating. The radon probe is located adjacent to hole W1. This decrease of the radon concentration could be either dilution by the interior house air being pumped into the wall cavity or dilution in combination with the increased wall cavity to basement pressure difference preventing the entry of the radon gas.

MITIGATION

An interim SSD mitigation system was installed at location V (the former 1.5 inch test hole) by making a 4.5 inch hole through the basement slab and installing 4 inch S&D pipe and a Kanalflakt model T2 fan. The mitigation system was exited through a basement window opening that had been covered with a clear polycarbonate sheet. A hole was cut through this sheet to allow the pipe penetration. The perimeter of the window and the pipe penetration were caulked to prevent the reentry of the radon. All joints in the pipe and fan were sealed. The flow in the mitigation pipe was 46 cfm with the fan on full speed and 1.465 inches of water suction was measured in the pipe 4.0 inches above the slab. The radon levels were reduced from a pre-mitigation average of 236 pCi/L to a post-mitigation average of 8 pCi/L in the basement. A corresponding decrease in the upstairs average level from 164 pCi/L to 10 pCi/L.

Although the average radon levels in the basement and living space were lowered by more than 90%, the HAC interaction still effects the radon levels in the same manner as before mitigation, figure 11. No sealing of the basement wall floor cracks or the furnace supply and return systems have been done at this time. The reasoning being that these procedures are irreversible and would be done at a later date after other experiments have been performed.

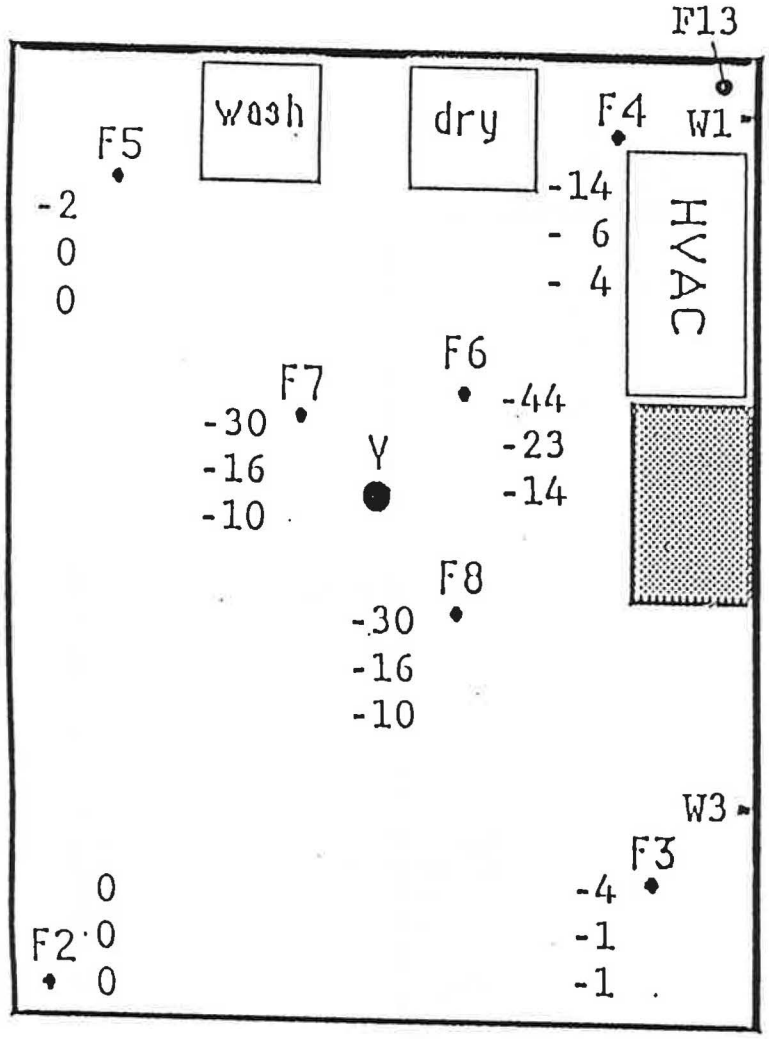

Figure 7. Pre-mitigation pressure differences between the subslab and basement measured during 2000, 1000, and 500 Pa suction pressures applied at hole V, house 21.

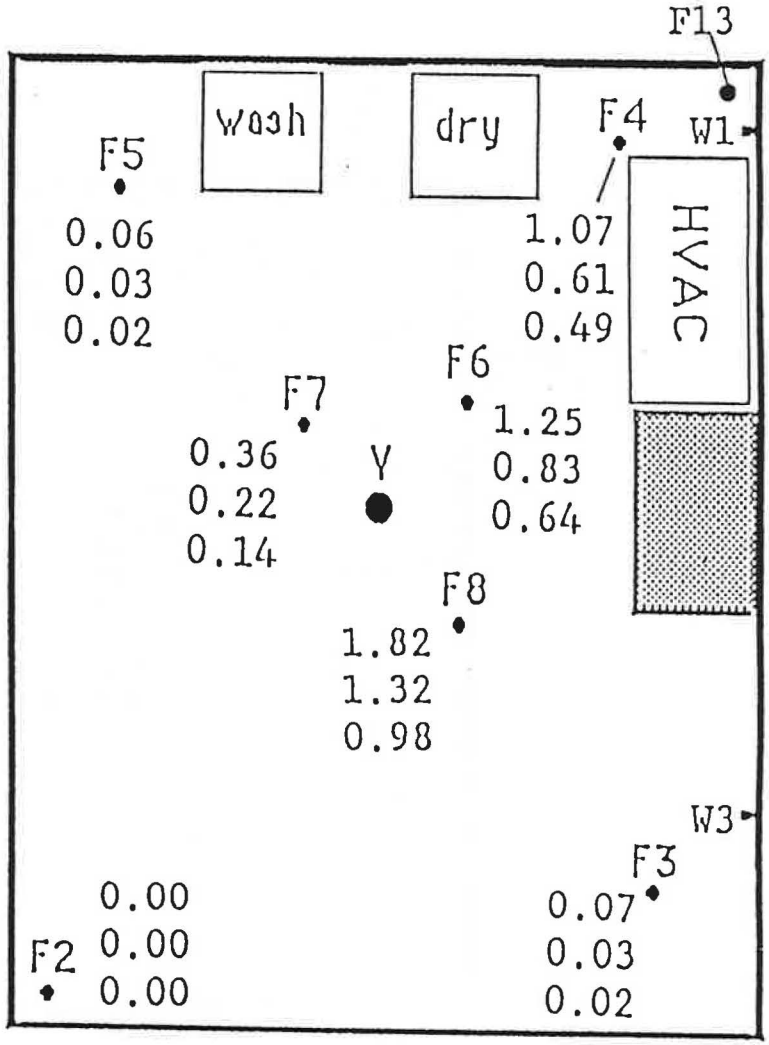

Figure 8. Pre-mitigation flow measurements through various subslab test holes during 2000, 1000, and 500 Pa suction pressures applied at test hole V, house 21.

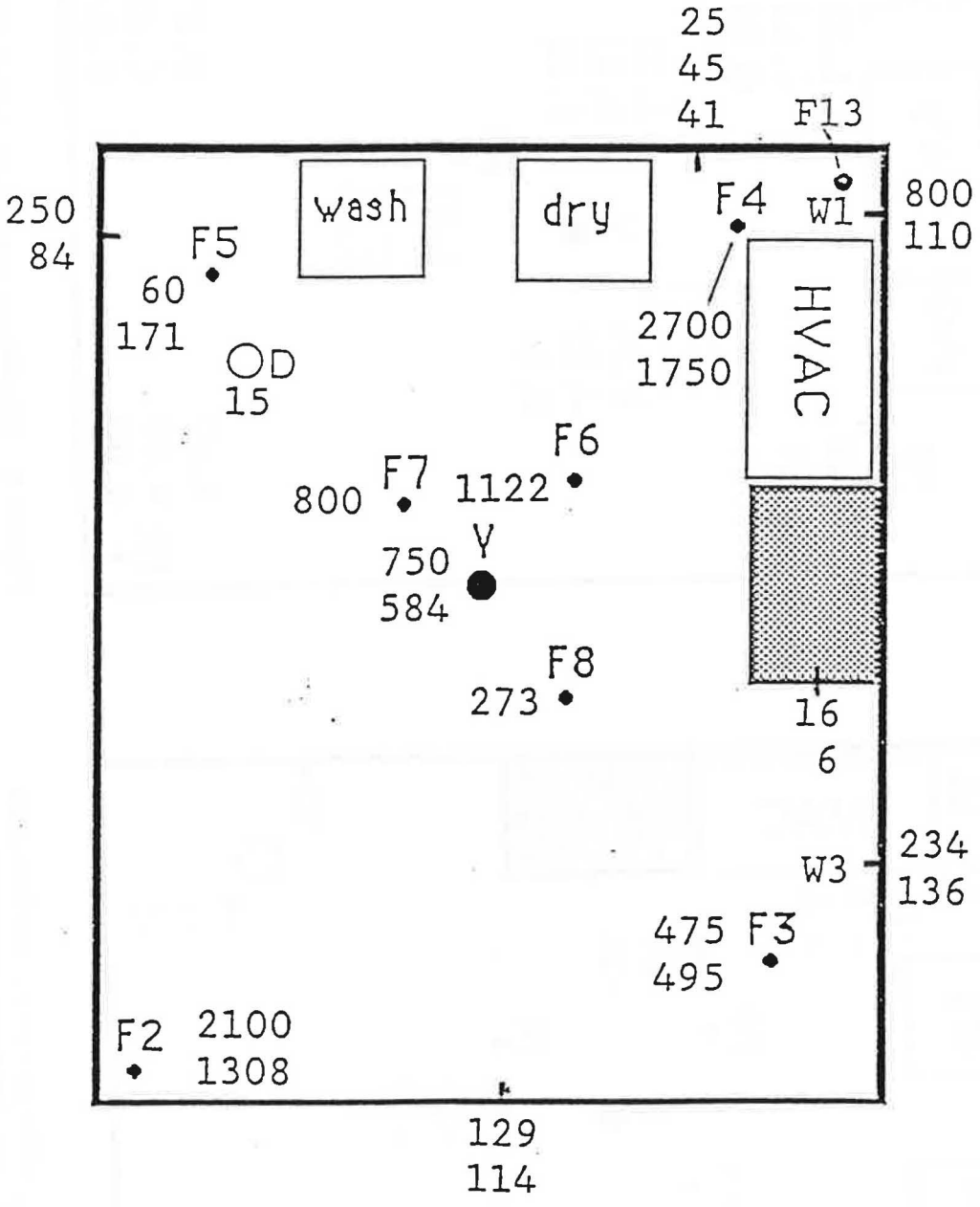

Figure 9. Pre-mitigation radon grab samples measurements from subslab test holes under ambient conditions, house 21.

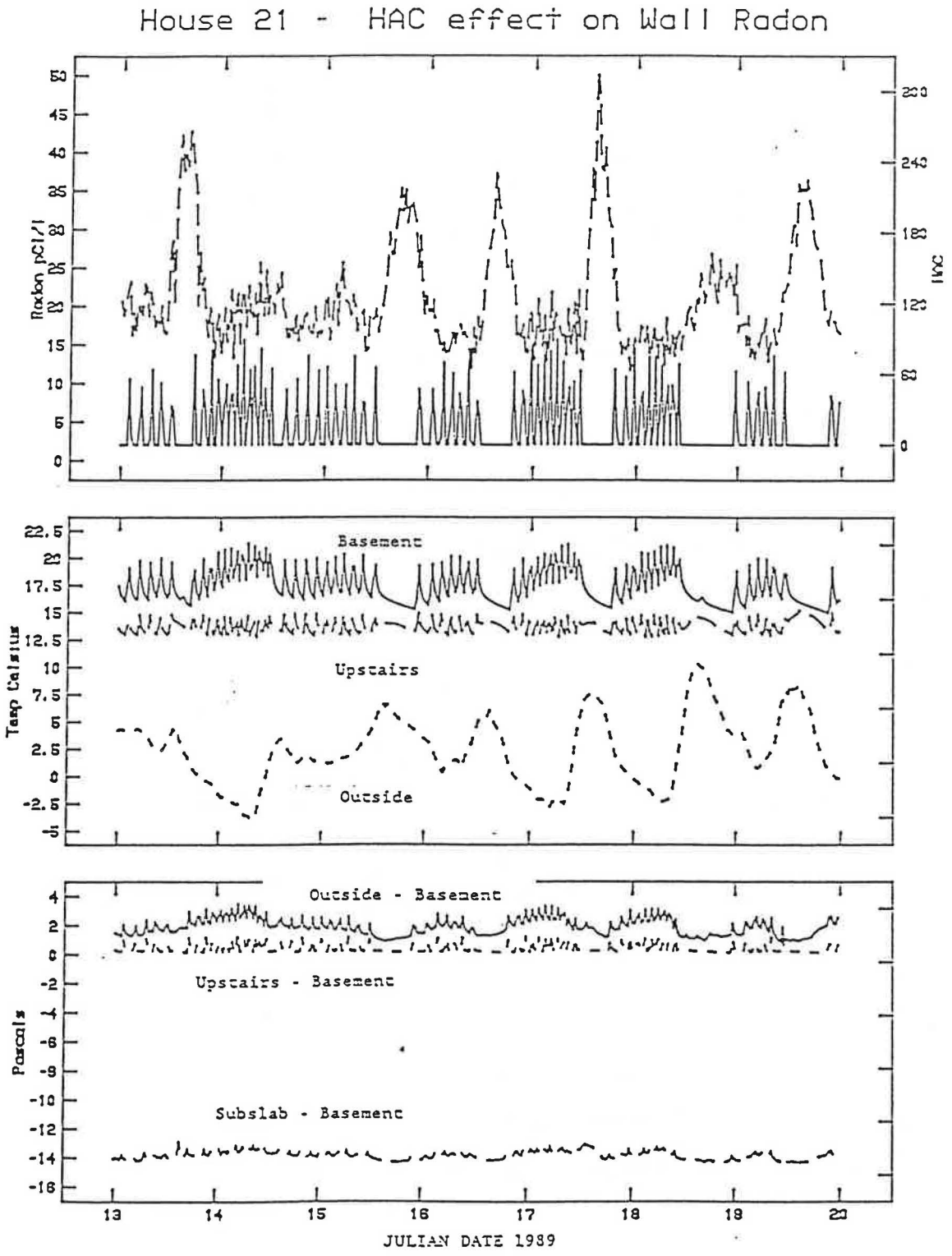

Figure 10. Wall radon concentration and HAC percent on time data, house 21.

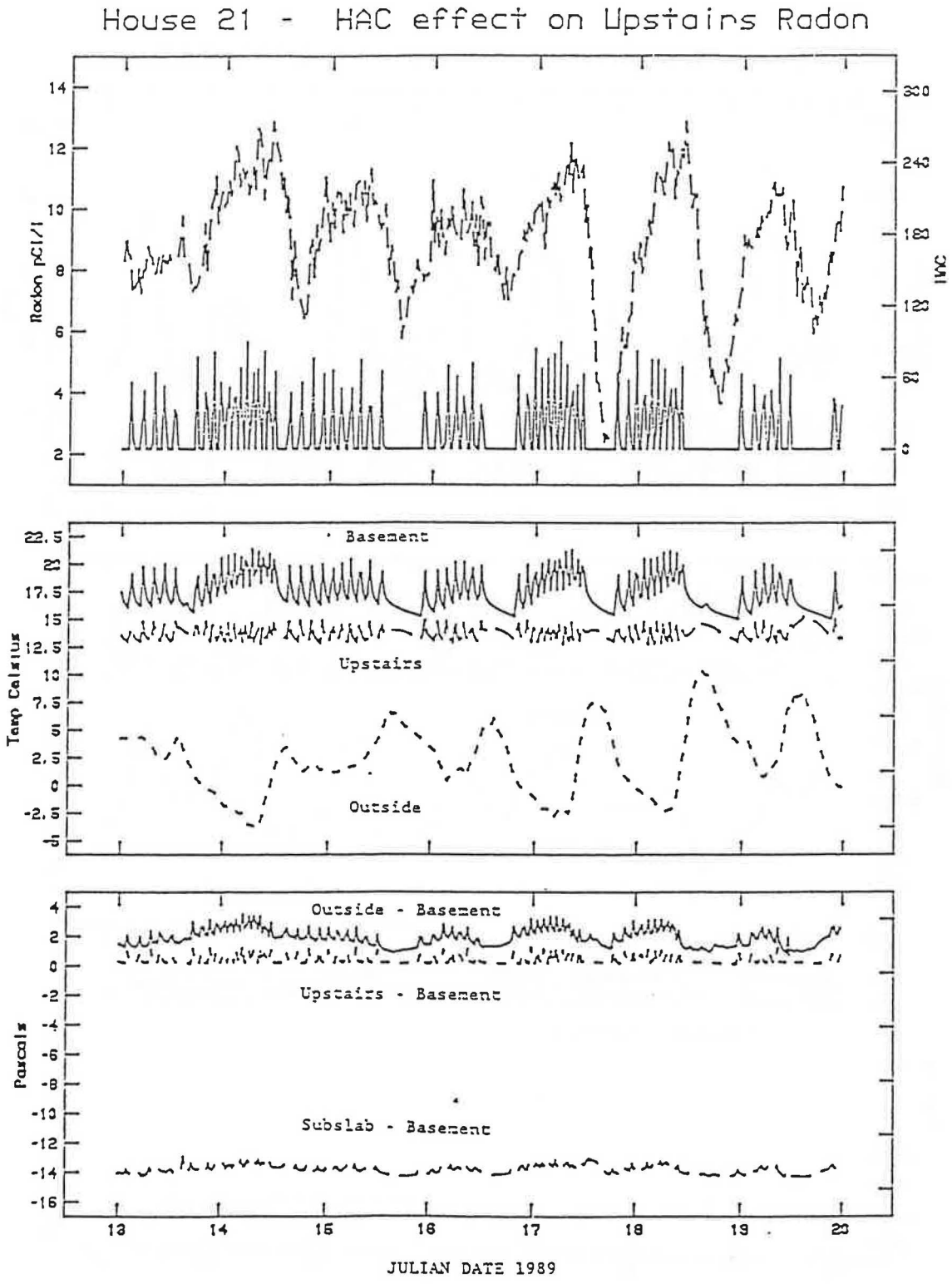

Figure 11. Post-mitigation upstairs radon concentration and HAC percent on-time, house 21.

PART C- AN APPROACH TO MEASURING DURABILITY IN RADON MITIGATION SYSTEMS

BACKGROUND

The subject of Durability of subslab depressurization systems used to mitigate radon problems in single family houses is just beginning to receive the much needed attention it deserves. The amount of data available on radon mitigation system performance over the long-term is very limited. In our study we are currently using a group of homes from the 1987-88 Piedmont Study as a sample-set to discover what takes place over the longer term. We have plans to add additional homes, supplied to us by the New Jersey Department of Environmental Protection. Those homes will be chosen from the 64% of mitigated homes[1] that have failed to remain below the 4 pCi/L radon concentration mandated in the EPA guidelines (mitigation was performed by certified mitigators as well as uncertified groups, including homeowners).

DATA COLLECTION

Our approach to evaluation of durability of the subslab radon mitigation system is based upon our own experience as to what might happen over time, as well as the experiences of others, e.g., NYSERDA efforts to quantify durability[2] and Swedish studies which were able to look at homes after five years of mitigation system operation[3]. Two short data sheets have been developed. One emphasizes the house and mitigation system as observed by the house occupants; the second involves a series of diagnostic tests which seek to determine whether or not the mitigation system is

achieving the radon mitigation goals.

Reviewing the data sheet, Radon Durability Diagnostics - I (Figure 1), the emphasis is initially placed on whether the system has been running steadily. Swedish studies have pointed to this problem as an explanation of radon concentrations climbing during their five-year monitoring[3]. Our own experience is that owners hate to admit to shutting off the system although AM radio interference and conserving electricity during the summer have been offered as reasons to turn the fan off. The second question concerns noise perceived by the home occupant. If the system is becoming noisy, our fear is that the fan may be "on its last legs," and/or that any noise may prompt occupants to shut the system down. A third inquiry involves moisture; here we are seeking information on condensation, collection of water in the mitigation piping or moisture-related events taking place at the roof exhaust. Water in the piping can directly influence the amount of exhaust airflow possible (or even stop airflow altogether). We have observed a complete cutoff of airflow due to accumulated water in one of our research homes. Condensation on the outside surfaces of the mitigation system can be another cause for occupants to turn the mitigation system off. The fourth question is aimed at finding out about possible power outages, construction in the home or other events that could affect the operation of the mitigation system and thus account for higher than expected radon levels. Question five is asked as an aid to detect any house settling and new radon leakage sites. Observations upstairs are viewed as possible clues to events involving the substructure. The final question involves the homeowner's perception of the system and whether they have questions about the way it functions. Knowing how the system functions can only help to keep the

system functioning properly.

The second data sheet, Radon Durability Diagnostics - II (Figure 2), emphasizes diagnostic procedures employed by the visiting inspection team. First there are the visible observations; for example, are there new cracks or places where radon might enter the house substructure? The inspection also concentrates on what sealing was done before and how well it has held up. The second item involves noise generation. Use of a stethoscope along the mitigation piping is aimed at better detecting early signs of bearing squeal and an indication that fan lifetime may be short. Item three is a diagnostic check of the airflow in the mitigation system piping. A heated wire anemometer inserted to the center of the plastic mitigation pipe is used to measure the air velocity. In the houses where the durability tests are in progress, openings in the piping are sealed with duct tape to provide easy access during diagnostic visits to the home. Care must be taken that the airflow probe is sealed where it enters the pipe to prevent erroneous airflow readings. Item four makes use of those same openings in the piping to evaluate pressure differentials. In this case our instrumentation is a digital electronic micromanometer and the measurement is in Pascals (although if the reading is in inches of water it is still more sensitive - four hundredths of an inch of water equals one Pascal). Item five deals with measurement of radon levels in the exhaust of the mitigation system. Over the long-term questions arise as to whether the radon is being depleted or perhaps that the soil is drying out, allowing the system to exhaust more distant radon gas with the result that radon levels may be raised accordingly. Both one-minute pumped samples and grab samples with Lucas cells are used in this testing; the Lucas cells are read using a Pylon. We

have just begun to collect such data. The one-minute hand-pumped Lucas cell samples (pumping exhaust air through the cell using a steady series of hand-pumping motions), have given higher readings than the evacuated Lucas cells - where an evacuated cell ingested the exhaust sample - this point will receive further attention as we make additional measurements of radon in the exhaust duct.

The final item in the inspection is to note general observations. This is an opportunity to note what a general inspection reveals, and what may influence the radon mitigation process. In this section, we have been also noting the serial numbers of alpha track detectors that were in place as well as the replacement detectors. As a first priority detectors have been placed in the basement/crawlspace areas as well as on the first floor.

An example of how these forms have been filled out for one of our houses is also included as Figure 3. Figure 3(c) shows the logging-in of radon detectors (and perhaps should also be formalized as data sheet III).

RADON DATA EVALUATION

Our experience in field visits to check the durability of subslab depressurization systems used to mitigate excessively high radon concentrations has now covered one year. The sample consists of six houses from the ORNL-Princeton segment of the Piedmont Study and two houses from the LBL segment. Three periods within this year have allowed us to quantify radon levels in the basement/crawlspace and first floors of each of the homes using alpha track radon detectors. At the end of each measurement period we have conducted the diagnostic tests just described.

First, it is useful to tabulate the radon concentrations in the eight houses over the year as shown in Table 1. This tabulation, when broken down

into average basement and first floor levels, for the six houses not experiencing a radon problem after mitigation, points to an interesting trend. Basement average radon concentrations are 3.28, 1.82 and 1.70 pCi/L for the three measurement periods (see Table 1). First floor average radon concentrations are 2.4, 1.78 and 1.44 pCi/L for those same periods. This decreasing trend, although based on a six-house sample, indicates a possible falloff of radon concentration over the year. Repeated test periods over the next year will allow us to determine whether these are long-term trends or possibly seasonal variations.

Two of the houses (house #3 and #5) have experienced an anomalous behavior, i.e., their first floor levels of radon reached the 0.6-0.8 pCi/L levels for the February-May 1988 period which was less than half the 1.78 pCi/L average of the other houses, yet during the Oct '87-Feb '88, and May-November '88 periods these radon concentration values were observed to be greater than the EPA Guideline, i.e., 4.7-4.8 and 8.4-6.0 pCi/L, respectfully (see Table 1). Basement levels were predictably higher at 8.35-8.0 and 11.6-9.8 pCi/L. Again, the values during the February-May 1988 period were 2.4 and 1.15 pCi/L (1.77 pCi/L average) respectively, slightly less than the 1.82 pCi/L average for the six houses which didn't have the problem of higher radon concentration reoccurrence. The fact that the six-house sample demonstrated a reduction in radon concentration over time, whereas these two houses exhibited a quite different behavior, necessitates a closer look into the individual house diagnostics.

Reviewing the general observations for house 3 and house 5, two items stand out. In house 5 this was the only homeowner who during good weather opened windows and turned off the radon mitigation system to save energy and

money. This was also the one homeowner who pointed to the mitigation system as the source of interference to the AM radio weather station he listened to each day. Again, the mitigation system was turned off briefly to remove the interference according to the homeowner.

The diagnostics in house #3 revealed new cracks, some 1/8" wide, extending for a number of feet toward the center of the floor. One other house had new cracks but certainly not of the same width as those in house #3. Additional diagnostics are needed to verify if this is actually the cause of the higher radon concentrations in period 3 and whether these cracks were overlooked in earlier inspection visits when this item wasn't emphasized in the diagnostic procedure.

Proposed in this contract period is the installation of timers to monitor time the mitigation system is in operation. Such monitoring will be initiated in these two homes in January 1989 together with a shorter time cycle on the alpha track replacement.

PRESSURE AND VELOCITY DATA

In each of the diagnostic visits, evaluation of pipe velocities and pressure drops have been the objective in data sheet II (Figures 2 and 3). These data have tended to be relatively constant over time for the majority of houses. Each of these measurements represents a reading at a given test point -- a "snapshot" of what is taking place.

Pressure levels at the various measurement points were typically found to vary from $\pm$1.4% to $\pm$15% except for house #3 which experienced over 30% variations in the readings (see Table 2). Lower readings were observed during the periods of higher radon concentration levels, e.g., for three test points, -18 and -28 Pa were found for the high Rn periods versus -39 Pa

for the low Rn period, -31 and -21 Pa for the high Rn periods versus -41 Pa for the low Rn period, and -40 and -25 Pa for the high Rn periods versus -51 Pa for the low Rn period. One question might be whether or not the fan setting had been adjusted even though the homeowner said it had remained unchanged.

Velocities in the mitigation system piping (Table 3) were found to be very stable over time for the majority of the measurement points (even zero changes) but with observed changes exceeding ±30% for others. One possible explanation is that velocity values were related to the wetness of the soil at or near the particular suction point. House #3 values varied between ±16.7 and ±22.2%. Although house 3 did not exhibit the greatest variation in velocity values, the pipe velocities were maximum during the low radon concentration period. For example, 1.68 m/s for the low period versus 1.2 and 1.50 m/s for the high periods; 2.04 m/s for the low period versus 1.3 and 1.58 m/s for the high periods; and 3.55 m/s for the low period versus 2.72 and 2.65 m/s for the high periods. The average velocity increase during the low radon period was 33%. Additional diagnostic tests this winter season most likely to be January (or February) and March (or April) should help to track the velocity variations more closely. We will try to determine whether cracks or soil wetness variations may be causing the system degradation.

CONCLUSIONS

The testing for durability of radon mitigation systems, even though our house sample is limited, has already pointed out some interesting trends and houses in trouble. Those homes which are not experiencing recurrences of radon concentrations above the EPA guideline would appear to be following a

long-term trend to lower radon concentrations in the basement and upstairs. As we add more houses to the data-set we will further check these observations which could be a result of radon depletion at the individual homesite. This may shed light on the question of soil dry-out and a possible wider reaching field for the subslab depressurization system.

The fact that two homes, which exhibit better than average radon mitigation performance in their "good" period, can then regress to above EPA guideline performance may give us insight to possible long-term problems. Turning off the system should be discouraged regardless of the window opening possibilities in warm weather periods. Does the presence of <u>new</u> cracks have anything to do with the presence of the subslab depressurization system? Are such tests pointing out how important new leakage sites can be in achieving radon reduction goals?

The addition of the NJ DEP homes to our database, and the installation of mitigation system down-time monitoring should help answer such questions during the coming year.

TABLE 1

Radon Concentrations in Eight Test Houses

HOUSE #	LOCATION	Radon Concentration pCi/L Oct '87 Feb '88	Feb '88 May '88	May '88 Nov '88
2	Basement	2.1	1.9	1.3
	Basement	2.4	1.3	1.0
	Floor 1 (Cabinet DR) (F-1)	-	-	0.6
3	Basement	6.8	1.2	7.6
	Basement	9.9	1.1	8.4
	Floor 1 (behind couch (F-1)	4.8	0.6	4.7
4	Basement	3.1	2.6	2.8
	Basement	3.0	2.3	2.8
	Floor 1 (LR Piano)	2.8	3.1	2.7
	(Breezeway) New			
5	Basement	11.6	0.7	9.8
	Floor 1 (MBR dresser)	8.4	0.8	6.0
6	Basement	5.1	1.9	1.7
	Basement C	4.8	2.8	2.3
	Basement under stairs	6.8	2.5	2.2
	Floor 1 (LR cabinet) (F-1) (near piano)	2.6	1.6	1.3
7	Crawlspace (1)	0.8	0.6	0.4
	Crawlspace (2)	1.0	0.3	
	Basement C	0.6	0.3	0.5
	Floor 1 LR Shelf	0.6	0.3	0.3
8	Basement	5.6	1.9	0.9
	Floor 1 (LR)	3.6	1.7	1.1
10	Basement	2.4	2.2	1.1
	Floor 1 (Study)	1.9	1.9	1.7

TABLE 2

Pressure as Measured in the Radon Mitigation Piping (Pascals)

House #	Oct '87-Feb '88	Feb-May '88	May-Nov '88	Percent Variation %
3	- 18 Pa	- 39 Pa	- 28 Pa	±36.8
	- 21	- 41	- 31	±32
	- 25	- 51	- 40	±34
4	- 105	- 114	- 98	±7.5
5	- 76	- 74	- 74	±1.3
	- 32	- 33	- 32	±1.5
	- 43	- 45	- 53	±10.4
	- 49	- 51	- 52	±3
6		- 100	- 106	±3
		- 47	- 52	±5.1
		- 82-90(-86)	- 89	±1.7
		- 62	- 66	±3.1
		- 89	- 93	±2.2
		- 73	- 75	±1.4
7	-30	- 42	-36	±16.7
	-32	- 38	-34	± 8.6
	-35	- 46	-44	±13.6
	-41	- 53	-56	±15.5

TABLE 3

Velocities Measured in the Radon Mitigation Piping (Meters per Second)

House #	Oct '87-Feb '88	Feb-May '88	May-Nov '88	Percent Variation %
3	.9-1.5 (1.2) m/s	1.68 m/s	1.50 m/s	±16.7
	1.1-1.5 (1.3)	2.04	1.58	±22.2
	2.0-3.45 (2.72)	3.55	2.65	±14.5
4	12.4	8.87	8.49 m/s	
5	4.5-5.2 (4.85)	4.26-4.7 (4.98)	4.2-4.7 (4.45)	±4.3
		2.2	2.03-2.19 (2.11)	±2.1
		3.39-3.52 (3.46)	3.30	±2.4
6		.83	.80	±1.8
		5.00	5.00	±00
		.04	0.1	±30
		2.3	2.15	±3
		3.8	3.30	±7
		2.2	1.2	±30
7	.95	1.55	1.6-2.0(1.8)	±30.8
	.40	.45	.38	±8.3
	.63	.80	.96	±20.6
	1.90	2.45	2.63	±16.1

REFERENCES

1. N. DePierro and M. Cahill, "Radon Reduction Efforts in New Jersey," Presented at the EPA Denver Meeting, December 1988.

2. I.A. Nitschke, M.E. Clarkin, T. Brennan and J.E. Rizzuto, "Long-term Assessment of Residential Radon-Mitigation Systems, " APCA, 1988.

3. I. Nilsson and P.I. Sandberg, "Radon in Residential Buildings - Examples of Different Types of Structural Countermeasures," Planning, Physics and Climate Technologies for Healthier Buildings, Swedish Counsel for Building Research, Stockholm, 1988, pp. 163-172.